CHALMERS
UNIVERSITY OF TECHNOLOGY

# How can corrosion damages be estimated based on surface observations?

Master's thesis in Master Program Structural engineering and building technology

Ahmad Uqla
Mojtaba Vafaeizadeh

Department of Architecture and Civil Engineering
CHALMERS UNIVERSITY OF TECHNOLOGY
Gothenburg, Sweden 2024

Master's thesis ACEX30 2024

# How can corrosion damages be estimated based on surface observations?

Ahmad Uqla , Mojtaba Vafaeizadeh


CHALMERS
UNIVERSITY OF TECHNOLOGY

Department of Architecture and Civil Engineering
*Division of Structural Engineering*
Research group: Concrete Structures
Chalmers University of Technology
Gothenburg, Sweden 2024

How can corrosion damages be estimated based on surface observations?
Ahmad Uqla, Mojtaba Vafaeizadeh



Supervisor: Professor Karin Lundgren, Postdoctoral researcher Langzi Chang, Department of Architecture and Civil Engineering
Supervisor from company: Valbona Mara, Afry
Examiner: Professor Karin Lundgren, Department of Architecture and Civil Engineering

Department of Architecture and Civil Engineering
Division of Structural Engineering
Research group: Concrete Structures
Chalmers University of Technology
SE-412 96 Gothenburg
Telephone +46 31 772 1000

Department of Architecture and Civil Engineering
Gothenburg, Sweden 2024

How can corrosion damages be estimated based on surface observations?

AHMAD UQLA, MOJTABA VAFAEIZADEH

Department of Architecture and Civil Engineering
Chalmers University of Technology

# Abstract

Reinforced concrete structures are widely used, but their lifespan is often shortened by reinforcing bar corrosion. Since concrete and steel production is resource-intensive and contributes to carbon emissions, enhancing the durability of existing structures can reduce material demand and environmental impact.

Visual inspections are largely based on surface observations. As corrosion progresses, the expansion of corrosion products increases the stress within the concrete, this stress leads to the formation of longitudinal cracks that run parallel to the bars. These cracks are a common and visible indicator of ongoing corrosion, signaling the need for further investigation. Several parameters affect the level of corrosion, including concrete cover thickness, bar diameter, concrete quality, and the ratio of concrete cover thickness to bar diameter.

This project focuses on investigating the relationship between the width of longitudinal cracks and the underlying factors influencing bar corrosion. Specifically, it analyzes the correlation between crack width and parameters such as concrete cover thickness, bar diameter, and concrete quality. Establishing these relationships is crucial for improving the accuracy of corrosion assessments and enhancing the ability to predict the remaining service life of reinforced concrete structures.

Keywords: Reinforced concrete structures, Corrosion, Visual inspections, Concrete cover thickness, Concrete quality, Bar diameter, Longitudinal cracks

# Acknowledgements

This thesis represents the culmination of our studies and research at Chalmers University, and it has been a rewarding journey filled with learning and growth. We owe a great deal of gratitude to those who have supported and guided us along the way.
Firstly, we would like to express our sincerest gratitude to Professor Karin Lundgren, who served as our supervisor and examiner. Her commitment to teaching and genuine care for her students have been instrumental in making this project possible. Her guidance and encouragement have greatly shaped our understanding and approach to the subject matter. We are truly grateful for her dedication and support.
We would also like to acknowledge the significant contributions of postdoctoral researcher Langzi Chang, whose unwavering support and vast expertise have been essential throughout the entire process of completing this thesis. His assistance has greatly enhanced the quality of our research.
This thesis was completed at Afry Gothenburg, and we are thankful to all the Infrastructure Division employees for their warm welcome and positive energy. A special thanks goes to our supervisor at Afry, Valbona Mara, for her invaluable guidance and support during our thesis work. Her time and effort have been crucial in helping us navigate and complete this project, and we are deeply appreciative of her assistance.
Finally, we extend our heartfelt thanks to our friends and family for their constant encouragement throughout our years of study at Chalmers. Their support has been a source of strength and motivation.
This thesis marks the end of an important chapter in our lives, and we are proud to leave Chalmers University with a wealth of knowledge, fond memories, and lifelong friendships.

Ahmad Uqla, Mojtaba Vafaeizadeh, Gothenburg, August 2024

# Contents

# List of Figures

# List of Tables

# 1
# Introduction

## 1.1 Background

Reinforced concrete is one of the most widely used materials for implementing civil engineering projects. Considering environmental concerns and existing guidelines aimed at reducing carbon dioxide emissions from construction projects, one of the solutions is to increase the lifespan of concrete structures [1]. One of the most significant reasons for the reduced lifespan of concrete structures is the corrosion of the reinforcement and its gradual loss of strength over time.

One of the clearest signs of understanding damages caused by corrosion in reinforcement bars is the presence of cracks resulting from corrosion and the spalling of concrete cover due to the increase in volume caused by corrosion products, which exert pressure on the surface of concrete and reinforcement bars [3]. Not all damages caused by corrosion are visible on the surface of concrete; it is possible for cavities to form on the surface of reinforcement bars without creating cracks on the concrete surface.In this case, the corrosion products typically fill the voids present in the concrete initially, which leads to a delay in the development of stress between the concrete and the rebar, and consequently, delays the onset of cracking [4]. Additionally, it is not easy to determine the extent of surface loss in reinforcement bars solely based on cracks resulting from concrete corrosion [5].

The corrosion process is divided into two stages: the initiation stage and the propagation stage [6]. At the beginning of the structure's service life, reinforcement bars' corrosion is prevented due to an alkaline environment in concrete. Cracks resulting from the corrosion of reinforcement bars lead to the loss of bond strength between the reinforcement and concrete. Additionally, the cracks increase the oxygen and hydrogen levels at the interface between the concrete and the reinforcement, raising the risk of corrosion in the reinforcement bars [7]. Furthermore, the resistance and ductility of reinforcement bars decrease due to the loss of cross-sectional area resulting from corrosion [8 and 9].

Cracks in concrete are a common occurrence and can result from a variety of factors, including shrinkage, thermal effects, and structural loading. These cracks provide pathways for corrosive agents, such as moisture and chlorides, to reach the embedded steel reinforcement. As a result, the width and nature of these cracks play a crucial role in influencing the rate of reinforcement corrosion [10].

Various studies have investigated the impact of crack width on the corrosion rate of reinforcement. Transverse cracks, for example, have been found to contribute significantly to the loss of cross-sectional area of the reinforcement, accelerating the corrosion process [11]. Longitudinal cracks, often induced by corrosion itself, also provide pathways for corrosive elements to reach the reinforcement, further influencing the corrosion rate [1].

Establishing an exact and universally applicable relationship between crack width and corrosion rate in reinforced concrete is challenging due to the numerous variables involved in the corrosion process. The relationship is highly dependent on various factors, including environmental conditions, concrete mix properties, the presence of aggressive substances, and the specific design and construction details of the structure [13].

Researchers have conducted numerous studies to investigate the correlation between crack width and corrosion level, and while some trends have been identified, no universally precise and deterministic equation exists. The relationship is often expressed in more general terms, and specific correlations may vary based on the experimental conditions and the specific parameters considered.

## 1.2 Aim

This thesis aims to assess the correlation between corrosion levels in bars and surface changes in reinforced concrete by comparing the data obtained from the visual inspection of existing structures and the outputs derived from previous studies. To achieve this objective, the following steps were taken:

- Analyze the data obtained from inspections conducted on existing structures.
- Investigate the influence of various parameters on corrosion and cracking.
- Categorize different types of cracks (Longitudinal and transverse) and choose one of them that is more correlated with corrosion level.
- Study the relationship between crack width and corrosion level and find a correlation between them.

## 1.3 Limitations

The limitations of this work are as follows:

- Lack of information related to the corrosion level of rebars in concrete from real data due to the visual inspection.
- Cracks other than longitudinal cracks were not considered.
- Insufficient data from samples with similar characteristics in experimental studies.

- Insufficient data of naturally corroded samples.

## 1.4 Methodology

The study examines previous research on corrosion in reinforcement bars, including the influencing parameters and the existing cracks in concrete, and their relationship with the level of corrosion. This investigation aims to gain a better and deeper understanding of the corrosion process in reinforcement bars. Additionally, it explores the formation of longitudinal cracks, their dimensional increase, and how these cracks contribute to increased levels of corrosion and their propagation in reinforced concrete.

Data obtained from the inspection of existing structures have been thoroughly examined, and interviews with inspection specialists conducted to gain a comprehensive understanding of common corrosion damages, their detection and classification methods, the causes of crack formation, and the mechanisms of crack propagation. The impact of these factors on the corrosion process has been investigated and categorized. Furthermore, a statistical study of previous research has been carried out, coupled with data collection on the width of longitudinal cracks and the extent of corrosion, followed by a detailed analysis.

# 2
# Literature study

## 2.1 Corrosion process

The corrosion of steel rebar in concrete due to chloride exposure is a significant concern impacting the durability of reinforced concrete structures. Corrosion of steel in concrete is an electrochemical process. The corrosion process in reinforced concrete starts with the concrete's highly alkaline pore solution, which creates a protective passive film on the steel reinforcement, that reduces the exchange of ions between the steel and the surrounding concrete. This film prevents corrosion as long as the PH remains high (PH 12.5-13.8) [30]. However, when chloride ions penetrate the concrete, they can break down this passive film, initiating corrosion. Chlorides can enter the concrete from contaminated materials or external sources like deicing salts. An electrochemical reaction occurs once the passive layer is compromised, causing the steel to corrode. This process is accelerated by factors like carbonation or further chloride contamination, leading to the deterioration of the reinforced concrete structure. Figure 2.1 shows the Chloride-induced corrosion process.

The corrosion produced by this phenomenon is typically identified by localized pits and extensive uncorroded regions, leading to significantly higher local corrosion rates compared to those initiated by carbonation. The ingress of chlorides into the concrete cover can occur through various transport mechanisms, broadly categorized as transport through porous media and transport through cracks. The primary defense against pitting corrosion is provided by both the passive film and the thickness of the concrete cover[3].

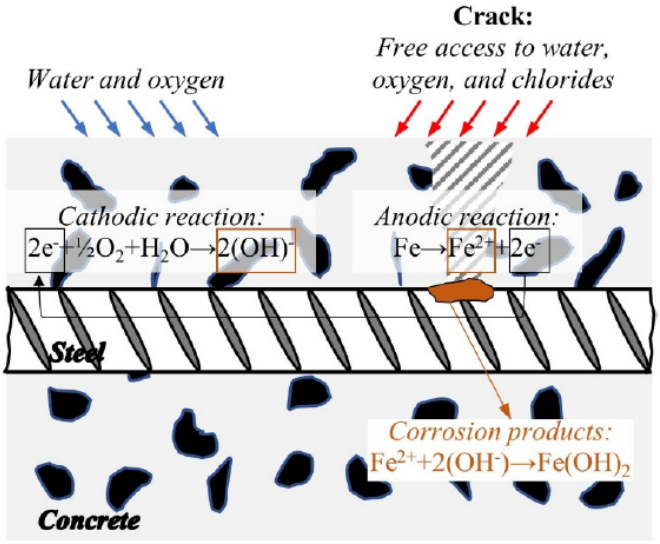


**Figure 2.1:** Chloride-induced corrosion process from [29]

It is expected that the accumulation of corrosion products at the steel/concrete interface will create expansive stresses, leading to the development of corrosion-induced cracks and spalling of the concrete cover. The extent of volumetric expansion in corrosion products is governed by the iron-to-rust ratio, a crucial factor in determining the duration from the initiation of corrosion to the formation of corrosion-induced concrete cracking. The iron-to-rust ratio for corrosion products without chlorides is anticipated to vary between 2.2 and 6.4, depending on the availability of oxygen and hydrogen during the formation of the corrosion products[19].

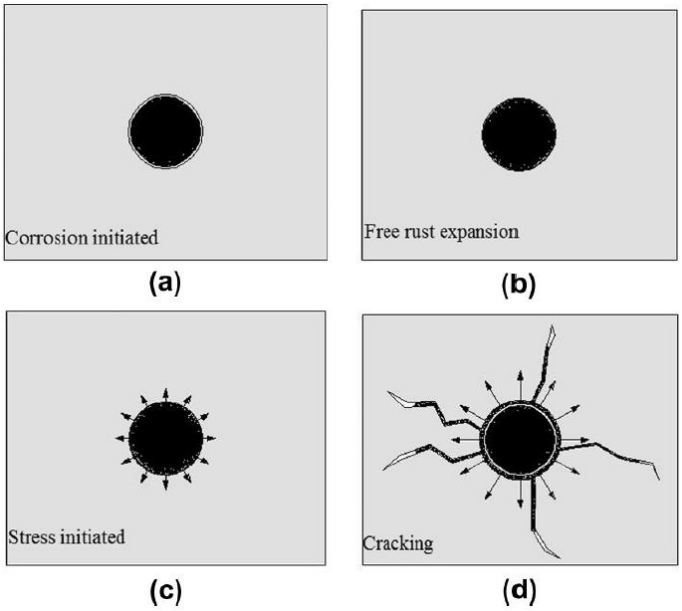


**Figure 2.2:** Effect of corrosion product on concrete [34]

Internal reinforcement corrosion can potentially be identified by surface observation, as the damage from reinforcement corrosion often appears through the development of surface cracks in the concrete element. These cracks result from tensile stresses generated by expansive rust oxides, induced by the loss of passivity. The rust formed functions as a gel, seeping through the cracks to reach the concrete surface. Nonetheless, the presence of stains on surfaces or indications of drainage from concealed areas due to corrosion signals the existence of damage.

Many studies focus on the corrosion process because it can have structural effects on Reinforced Concrete (RC) structures, often resulting in a loss of safety and function for the structure [29].
To achieve this, researchers frequently employ artificial corrosion methods to replicate real-world corrosion conditions in the lab. Many corrosion models are based on results from these methods. Techniques like impressed current are favored because they significantly reduce the time required for the specimens to undergo corrosion [31].

## 2.2 Corrosion Mechanism and Corresponding effect on structures

Figure 2.3 presents the corrosion mechanism, bending and shear capacities are reduced due to the rebar cross-section reduction, a decrease in effective depth due to spalling of the concrete cover, and changes in bond conditions. Crack widths and deflections are affected due to changing tension stiffening linked to the degraded bond. The deformation capacity of the structure is impaired by highly localized damage, leading to a concentration of deformation. More severely, corrosion may change the failure mechanism from ductile, as designed, to brittle [30].

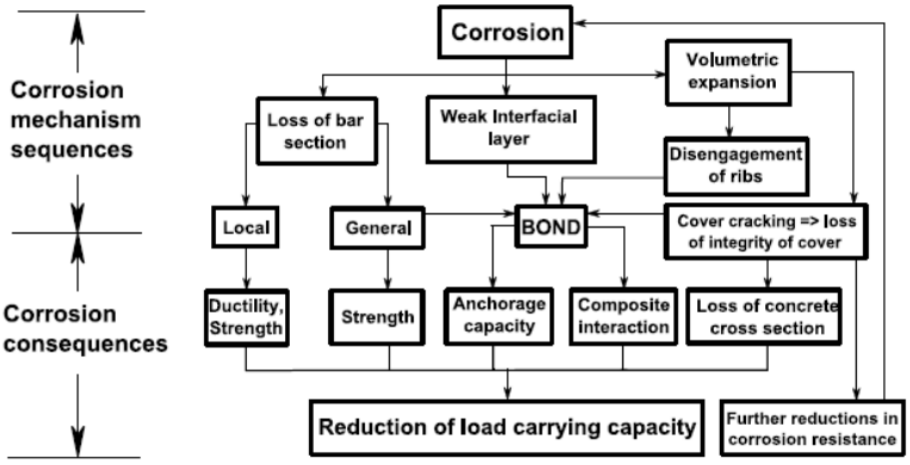


**Figure 2.3:** Corrosion mechanism from [34]

Corrosion affects RC structures in two main ways:

1. Corrosion changes the shape of the reinforcement bar by reducing its cross-sectional area. This leads to a decrease in its mechanical properties, strength, and flexibility [29].

2. Corrosion products generally take up more space than uncorroded steel. This creates pressure between the bar and the surrounding concrete. As corrosion products continue to be produced, this pressure can cause cracking and later, spalling of the concrete cover.[3]

Numerous studies cover various structural effects of corrosion, ranging from effects on reinforcement bars [8], [9] to the serviceability state, where corrosion affects deflections, stiffness, and, consequently, load redistribution, to the ultimate state, where the effects on load-carrying capacity as shown in figure 2.3 are studied in terms of bending capacity, shear capacity, and anchorage [31],[34].

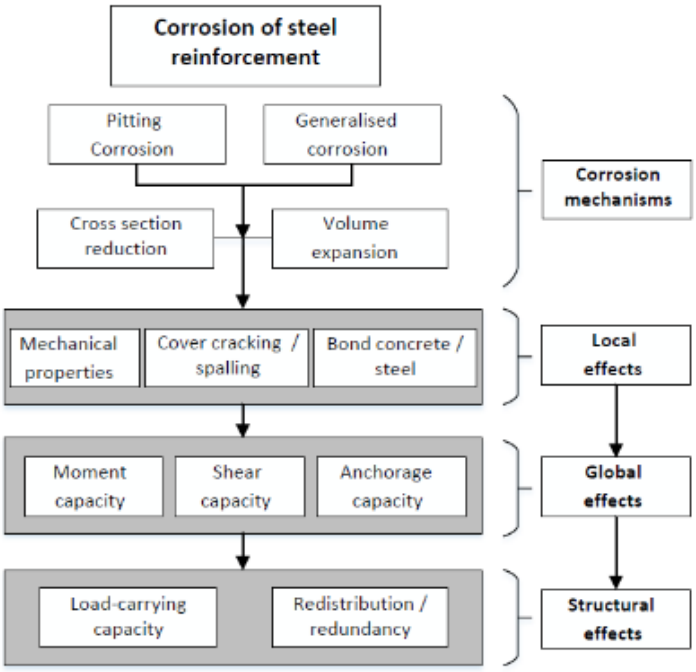


**Figure 2.4:** Effect of corrosion on load-carrying capacity from [34]

## 2.3 Pitting corrosion

Concrete reinforced Structures exposed to chloride environments often experience pitting corrosion on their rebars. This type of corrosion is particularly concentrated and localized, leading to a notable reduction in the cross-sectional area. Several factors influence the uneven distribution of pitting corrosion, such as the bar's position during casting, the occurrence of cracks due to early stress or loads, imperfections

at the steel-concrete interface, and variations in the metallurgy and concrete quality. Consequently, this localized loss of material can lead to decreased ductility in the reinforcing bars, caused by irregular cross-sectional distribution and the stress concentrations that occur due to sudden changes in the bar's geometry [29].

Pitting corrosion is localized, deep pits on a bar surface, significantly increasing the corrosion rate in these specific areas. While the overall corrosion rate provides an average measure of material loss over time, pitting corrosion causes a much higher localized corrosion rate at the pits, which can lead to premature failure.

Several factors impact the rate of corrosion: in uncracked concrete, the initiation of corrosion-induced cracks, followed by subsequent spalling of the concrete cover, accelerates the corrosion process. Conversely, in cracked concrete, self-healing of cracks may decrease the corrosion rate by limiting the flow of aggressive substances. Additionally, seasonal variations and alterations in the exposure environment can also affect the corrosion rate [29].

Cracks in structures can help corrosion products move away from the steel/concrete interface [29]. Additionally, the compressibility of rust itself is a significant factor that delays the time it takes for the concrete cover to crack [29].

## 2.4 Concrete cover

When looking at bending cracks, the width of bending cracks on the surface usually increases as the concrete cover thickness increases, assuming the crack opening at the steel-concrete interface remains the same. Increasing the thickness of the concrete cover is expected to delay both the start and spread of corrosion. However, choosing a thinner concrete cover may be beneficial in decreasing surface crack width. If there are no cracks, it prevents chlorides from reaching the reinforcement bars through the pores. When cracks are present, concrete cover depth delays the penetration of corrosive agents to the rebar surface, thereby reducing the corrosion rate [16,18].

## 2.5 Impressed Current

In accelerated corrosion investigations, the impressed current technique is employed to expedite tests within a practical timeframe. Corrosion is induced by applying an electrochemical potential between the anode of the reinforcing steel and a cathode.

The impressed current technique typically utilizes Faraday's law to theoretically calculate the mass loss of reinforcing steel [13]. In the theoretical determination of corrosion mass loss through the application of Faraday's law, the assumption was made that the impressed current exclusively contributed to the corrosion reaction, generating all ferrous ions on the anode. Nonetheless, previous research has

revealed inconsistencies between experimental results obtained through the gravimetric method, 3D scanning process, and transmission imaging technique for mass losses in reinforcing steel and the theoretical outcomes derived from calculations based on Faraday's law [13].

Employing various current densities had no impact on the mass loss percentage [13]. Nevertheless, elevating the current density beyond 200 mA/cm$^2$ led to a notable escalation in the strain response and crack width, attributed to the corrosion of the steel reinforcement [17].

In past studies, the strengths of impressed electric currents ranged from 45 to 10400 mA/cm$^2$[17]. Observations suggest that when corrosion reaches similar levels, higher electric currents are linked to a significant rise in crack width [17]. Lower electric currents require a longer time for corrosion compared to higher ones to reach the same amount of rust. This extra time allows rust to spread into the pore system in the concrete, easing the pressure around the steel bars and resulting in smaller cracks [13]. Also, when employing an impressed current, the entire bar functions as an anode, typically leading to overall corrosion along its entire length. Moreover, the potential difference between the anode and cathode is usually several times greater in impressed current applications compared to the natural process. This disparity affects both the spatial distribution and composition of the corrosion products [32].

## 2.6 Concrete Quality

The quality of concrete significantly affects the corrosion in reinforcing bars. When the concrete has fewer voids and cracks, and is denser, its quality is higher. Higher density makes it harder for harmful substances to penetrate the concrete, thus delaying the onset of corrosion in the steel bars. However, the same increase in strength can make the concrete more brittle, which might lead to more cracks. These cracks increase pathways that allow corrosive agents such as chlorides to reach and damage the reinforcing bars[3].

Moreover, the PH level within the concrete is crucial for protecting against corrosion. Concrete with higher strength typically maintains a higher PH because it contains extra calcium hydroxide, a byproduct from when cement hydrates. This high PH creates a protective environment around the steel bars by forming a barrier layer, which helps prevent corrosion. Thus, while high-quality concrete can offer better resistance to the penetration of corrosive agents due to its lower permeability, its increased brittleness and potential for cracking must also be considered in managing its overall protective properties against corrosion[32].

The cover quality is determined by concrete properties, with the water/binder ratio typically considered the primary influencing factor in concrete containing ordinary Portland cement. Many studies have explored how cover thickness and water/binder ratio impact the corrosion process [18].

Lowering the water/binder ratio has been linked to higher concrete resistivity, reduced oxygen penetration, and increased alkalinity, all of which are expected to lower the corrosion rate [18].

## 2.7 Loading Type

Under constant loading, the cracks are spaced closer together than in dynamic loading scenarios, leading to a modification in the concrete environment and its transformation into a cathodic area. This transformation results in a reduced pitting corrosion rate, consequently decreasing the production of rust products and lowering the stresses between the reinforcing bars and the concrete. Furthermore, dynamic loading has the potential to dislodge debris and self-healing substances from cracks, potentially causing additional damage at the steel-concrete interface [11].

## 2.8 Self-healing

Self-healing is anticipated primarily in marine structures, where cracks may see precipitation of magnesium hydroxide and calcium carbonate [12]. Structures exposed to de-icing salts, which provide chlorides, also have the potential for self-healing. However, in this case, the self-healing is likely due to debris or corrosion products blocking the cracks [32]. The incorporation of self-healing mechanisms can enhance resistance to chloride ingress in the presence of cracks [32].

## 2.9 Cracks

Concrete structures commonly develop cracks because of their limited tensile strength. These cracks can be categorized as either non-structural or structural. Structural cracks are usually wider than 0.1 mm, while non-structural cracks are generally finer. Structural cracks often occur due to insufficient reinforcement, low concrete strength, excessive loading, or permanent actions such as foundation settlement and creep. Non-structural cracks may result from physical factors such as shrinkable, and thermal impacts[3]. Figure 2.5 illustrates the different types of cracks and their origin.

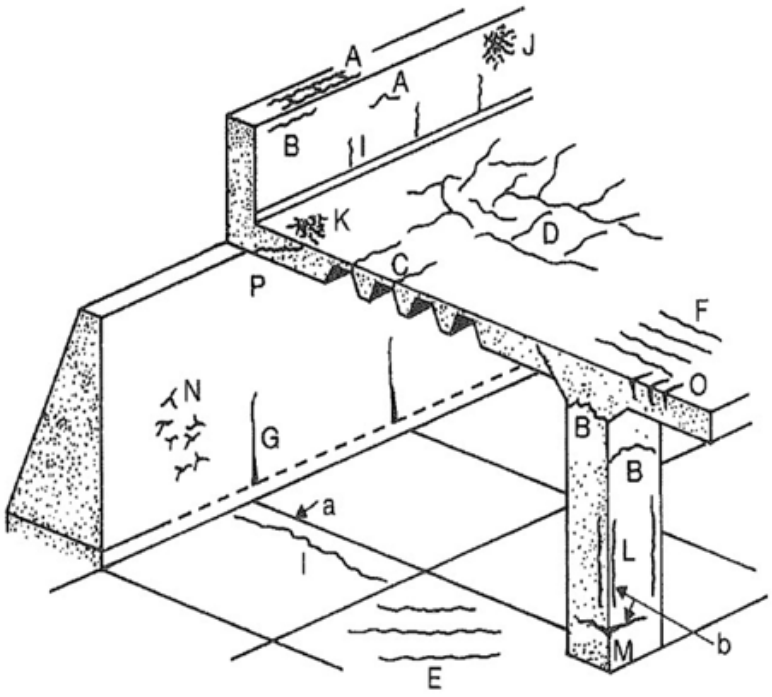


A- Plastic settlement crack, above reinforcement
B- Plastic settlement crack, at arch formation
C- Plastic settlement crack, at change in thickness
D- Plastic shrinkage crack, irregular
E- Plastic shrinkage crack, parallel
F- Plastic shrinkage crack, above reinforcement
G- Thermal crack, through
H- Not specified
I- Shrinkage crack, due to external restraint
J- Craze cracking, towards form surface
K- Craze cracking, after surface treatment
L- Reinforcement corrosion cracks, due to carbonation
M- Reinforcement corrosion cracks, due to chlorides
N- Alkali-aggregate reactions
O- Load-induced cracks, bending crack

**Figure 2.5:** Different types of cracks and their origin from [5]

### 2.9.1 Transverse cracks

The general agreement in the literature is that the existence of transverse cracks typically shortens the time to corrosion initiation[28]. This is primarily due to the cracks providing a preferred pathway for potentially harmful substances, such as chlorides and carbon dioxide, to reach the reinforcing bar. Controlling the width of surface cracks is anticipated to reduce the influx of these substances to the reinforcing bar, thereby extending the service life of the structure [33].

Surface crack width is controlled by codes to restrict the corrosion of reinforcement bars within concrete. Transverse cracks serve as reliable indicators of the location of corrosion pits, with the corrosion rate of the pits escalating near cracks. Over time, pits exhibit a slower growth rate in-depth but their number increase. Despite this, no distinct correlation between surface crack width and corrosion damage has been established. Bending frequently induces transverse cracks, with cracks formed through bending generally exhibiting greater widths at the surface compared to the reinforcement level [32].

### 2.9.2 Longitudinal cracks

As illustrated in Figure 2.5, the longitudinal cracks originate from corrosion in the reinforcement. The presence of rust between the steel and concrete leads to the development of longitudinal cracks as a result of corrosion. With the advancement of corrosion, these cracks can lead to the detachment of the concrete cover. These cracks serve as clear indicators of ongoing corrosion in the steel reinforcement [7].

According to previous studies, determining the most corroded section solely by examining the width of longitudinal cracks is not possible, consistent with the findings of [7], [11]. Longitudinal cracks did not start forming at sections with a higher local corrosion level. Instead, in most cases from the artificial method, new cracks were observed to develop in the areas between transversal cracks and these regions had relatively low corrosion levels. This observation could be explained by the movement of corrosion products through open transversal cracks, caused by applied loads. This release of stress helped alleviate the pressure from the rust accumulation in the cracked sections.

On the contrary, in areas without transversal cracks, even though they showed a visibly lower corrosion level, the absence of cracks confined the corrosion products, leading to increased stresses and earlier crack initiation. This observation emphasizes that the mechanical impact of corrosion products plays a more crucial role in corrosion-induced cracking than the actual extent of corrosion itself [7].

A relationship exists between longitudinal cracks and pit volume. Longitudinal cracks result from the buildup of corrosion products. Simultaneously, as these cracks expand, more steel surfaces become exposed to chloride, initiating corrosion and leading to an increased loss of rebar volume. [11]

Typically, the pits beneath longitudinal cracks experience more significant volume loss compared to those without such cracks. This can be attributed to the larger surface area of steel exposed to the external environment when a longitudinal crack is present, in contrast to a transverse crack. According to E.chen et.al [11] when the longitudinal cracks are wider, there is more corrosion in most pits. However, in some severe cases, these pits do not create long cracks, or if they do, the cracks are very small. It is crucial to understand that not every pit with corrosion results in

longitudinal cracks. Therefore, in practical situations, the width of the longitudinal cracks may not get an accurate measurement of the extent of corrosion in pits.

## 2.10 Discussion

According to the literature study, various parameters influence the corrosion level and the formation of cracks. Visible surface cracks, which are quantifiable, indicate underlying corrosion attacks. Generally, the width of these cracks correlates with the extent of reinforcement corrosion and the bar density in the affected area. Analysis of experimental data from existing literature clearly shows a correlation between the width of these cracks and the severity of corrosion, though a quantified correlation has not been found. This study aims to estimate the corrosion level in rebar based on visual indicators. Therefore, it focuses on parameters that are quantifiable without the need for taking samples and laboratory work. Considering the mentioned parameters, four parameters including the thickness of the concrete cover, the concrete quality, the size of the rebars, and the width of longitudinal cracks are selected to establish a relationship.

# 3
# Practical engineering case studies

In this chapter, reports of several case studies conducted by specialists from Afry Company were examined, each with a different structure and exposure to various environmental conditions. Interviews with inspection experts were conducted to understand the criteria for selecting inspection points, identifying significant damages, prioritizing areas for inspection, signs of corrosion, methods of measuring cracks, and other relevant factors.

All inspections carried out by Afry specialists were visual, focusing on parts of the structures with more cracks, discoloration, or concrete delamination. According to the interviews, a common method for assessing corrosion levels in rebars is measuring the chloride content present on the rebar's surface. The chloride concentration needed to initiate the corrosion process is often called the chloride threshold value. This value varies in the research literature and is influenced by factors such as oxygen availability and moisture. As a reference, the chloride threshold value can be obtained from Table 3.1.

**Table 3.1:** Assessment of chloride content in uncarbonated concrete from [42].

| Chloride concentration ( of cement weight) | Probability of corrosion |
|---|---|
| Less than 0.4 | Negligible |
| 0.4-1.0 | Possible |
| 1.0-2.0 | Probable |
| More than 2 | Certain |

The table is based on empirical values from laboratory experiments in a marine environment. According to Table 3.1, based on the chloride content present, inspectors cut opening windows for further examination of the condition of rebars embedded in the concrete. In some cases, samples were sent to the laboratory for chloride content determination.

Visual inspections identified signs such as cracks wider than 0.2 millimeters according to Eurocode, color changes in concrete due to liquid discharge from corrosion, or surface deterioration due to increased stress between the reinforcement and concrete caused by the volume increase from corroded reinforcement materials. In this type of inspection, the method of measuring cracks is mostly based on a crack ruler which is shown in Figure 3.1. Due to limitations in crack detection, this measurement method

is not sufficiently accurate, leading to potential human errors.

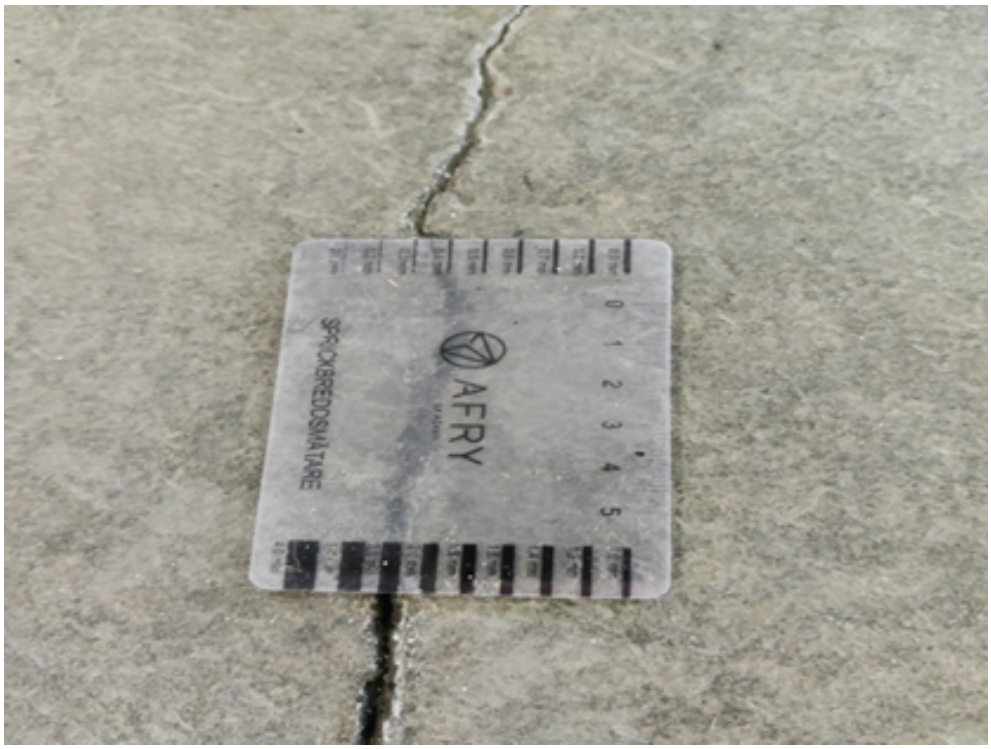


**Figure 3.1:** Crack ruler (Common method for measuring cracks) from Afry reports.

Before studying any of the cases, questions were prepared to be asked of the inspection specialists, which are compiled below:
1. What indicators are important to you in the inspection process?
2. In which part of the structure are the rebars most susceptible to chloride-induced corrosion?
3. What tool do you use to measure the width of cracks?
4. What method do you employ to detect corrosion in the rebars?
5. Is there an instrument available on-site for measuring corrosion in the rebars, or is the extent of corrosion estimated approximately?
6. What is the reason for opening multiple adjacent windows during inspections?
7. What method do you use to detect delamination in concrete?
8. How do you ensure that cracks are due to corrosion? Are periodic inspections conducted, and are the findings meticulously recorded?
9. What is the duration of periodic inspections for each structure? Do you provide a schedule to the owner, or does the owner request inspections based on the structural conditions?
10. Is there any specific regulation mandating the inspection of structures at regular intervals?
11. How do you proceed when repairs have been made on the concrete surface and signs of corrosion have disappeared? Do you reopen windows and inspect the rebars again?
12. How important is the thickness of the concrete cover in inspections?

13. How significant is the role of surface coatings like asphalt or other materials in delaying corrosion?
14. What effect does the type and strength of concrete have on the rate of corrosion?
15. How do the size and number of rebars influence corrosion?
16. What is the typical water-to-cement ratio in the structures you inspect?
17. How do you perceive the impact of loading type, specifically dynamic loading, on the structure?
18. How influential are the environmental conditions and humidity levels on the structure?

Following the interviews with the specialists, the questions mentioned were asked, and the responses provided are detailed below:

According to regulations for infrastructure structures related to the Trafikverket agency, the duration of periodic inspections is every six years, which may be adjusted based on the structure's condition. In other structures, inspection schedules depend on the owner's request and vary depending on the structure's age, exposure conditions, and prior inspection findings. A schedule is typically provided to the owner, but inspections can also be requested based on observed structural conditions. Environmental conditions and relative humidity levels are also highly influential, as high relative humidity and aggressive environments (e.g., marine or industrial) can significantly accelerate corrosion processes.

Key indicators of deterioration in reinforced concrete include visible signs such as discoloration, cracking, spalling, and rust stains. Additionally, measurements of concrete cover thickness, crack width, and chloride content are crucial. Rebars are most susceptible to chloride-induced corrosion in areas exposed to deicing salts, marine environments, and where water ingress is prevalent, such as joints, cracks, and surfaces with inadequate concrete cover.

Crack width is typically measured using a crack ruler, and corrosion in rebars is detected using methods that identify surface changes like discoloration, cracking, spalling, and rust stains. Delamination is detected using hammer test methods. Ensuring that cracks are due to corrosion involves periodic inspections and detailed visual assessments.

The thickness of the concrete cover is crucial, as it directly influences the protection of the rebar against corrosion; insufficient cover increases the risk. Surface coatings can significantly delay corrosion by providing an additional barrier against water and chloride ingress, though the effectiveness depends on the quality and maintenance of the coating.

The quality of concrete affects its permeability and resistance to chloride penetration, with high-quality, low-permeability concrete typically having a slower rate of corrosion. Closely spaced rebars can create areas where chloride ions accumulate, increasing corrosion risk. Dynamic loading can lead to fatigue and microcracking,

accelerating the ingress of corrosive agents and increasing the rate of corrosion. Subsequently, each case was individually examined, aiming to find the relationship between crack width and corrosion levels.

## 3.1 Case Study One

Case One is a multi-level parking structure built in 1973. The structural system consists of columns, main beams, and concrete slabs. The inspection, based on the Swedish Transport Administration's protocols, classified damages according to functional conditions (see Table 3.2). Inspections were limited to accessible areas, and in some cases, windows and concrete tributaries were opened to observe reinforcement conditions.

**Table 3.2:** Condition Classes for Assessing Functional Condition from [43].

| Condition class | Functional assessment |
|---|---|
| 3 | Deficient function at the time of inspection |
| 2 | Deficient function within 3 years |
| 1 | Deficient function within 10 years |
| 0 | Deficient function beyond 10 years |

Chlorides primarily reach the rebars through two pathways: one via vehicle tires and de-icing salts, and the other due to chloride content present in the cement, depending on the construction time of the parking lot. Inspections covered upper and lower concrete slab sections as shown in figure 3.2. The upper section exhibited corrosion-related damages such as cracking, concrete spalling, reinforcement corrosion, and accumulation of corrosion by-products. In the lower section, there was less damage, likely due to the lower proximity of harmful materials from passing vehicles.

**Figure 3.2:** Cracks and concrete spalling in the upper section from Afry reports.

It's important to note the composition of each floor, as some floors have asphalt layers, providing additional protection against harmful substances, delaying corrosion, and reducing its impact.

### 3.1.1 Inspection on the first floor

In order to examine the corrosion status in concrete, after inspecting visible signs such as crack width and concrete spalling, and conducting a rebound hammer test to detect concrete delamination, windows were opened to further examine the rebars for a more detailed inspection.

Window F3 was situated in a parking area adjacent to a large structural column, spanning both primary and support beams. Upon tapping the road surface, indications of delamination were audible. To assess the condition of the underlying concrete, careful excavation through the road surface and insulation layers was conducted. Subsequently, the metal reinforcement bars from the concrete were extracted. Findings are summarized in Table 3.3, and visual documentation of the exposed reinforcement is provided in Figures 3.3 and 3.4.

In this window, the impact of the protective surface layer is clearly visible. This layer prevents harmful substances from reaching the rebar surface, resulting in the rebar remaining in good condition. Additionally, the thickness of the concrete cover is appropriate, which is another reason for the delay in harmful substances reaching the rebar surface and initiating the corrosion process. In fact, the surface layer acts as a shield against corrosive materials and potential damage, ensuring the structural concrete remains intact.

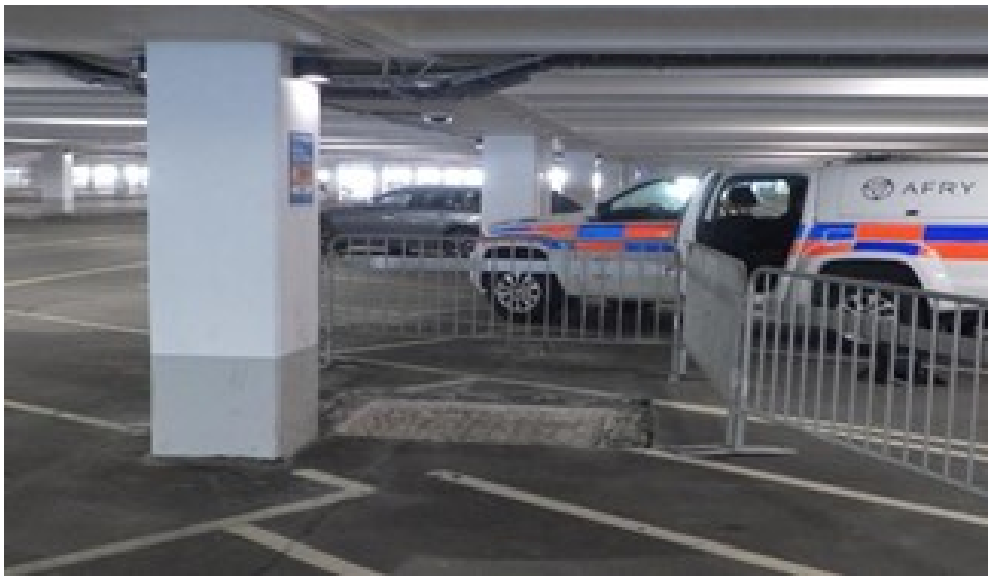


**Figure 3.3:** Location of window F3 from Afry reports.

**Figure 3.4:** Reinforcement status in window F3 from Afry reports.

**Table 3.3:** The measured parameters is relation to window F3.

| Parameter | measurement notes from examination of F3 |
|---|---|
| Cast asphalt + Insulation mat | Thickness 40mm |
| Overlay (hard concrete) | Unreinforced, thickness 40-70 mm. Probably executed for slope buildup. The overlay was delaminated and lacked adhesion to the structural concrete. There were also through cracks in the overlay, however, no cracks in the underlying structural concrete. |
| Reinforcement $\phi 8, S100(upperlayer)$ | Corrosion level: Generally healthy reinforcement, individual rebars with some millimeters of corrosion attack (difficult to measure). |
| Main reinforcement $\phi 16$ | Corrosion level: 2 visible and healthy rebars without corrosion attack |
| Concrete Cover layer | 30 |
| Other | Structural concrete without delamination. Initial delamination areas during the initial inspection are likely due to delamination of the overlay without adhesion |

Similarly, Window F4 was positioned in a comparable location near a column where delamination of the road surface was observed. Excavation through the road, insulation, and covering layers until reaching the concrete substrate is conducted, as illustrated in Figure 3.5. The outcomes of the investigation are detailed in Table 3.4.

In this window, the overlay thickness is less than in window F3, which could be one of the reasons harmful substances have reached the rebar surface, causing corrosion. Additionally, damage to the structural concrete has provided an easier path for more harmful substances to penetrate, accelerating the corrosion process. The impact of cracks is also clearly visible in this window, with corrosion occurring precisely near the cracks.

**Figure 3.5:** Location of window F4 from Afry reports.

**Table 3.4:** The measured parameters are related to window F4.

| Parameter | Measurement notes from examination of F4 |
|---|---|
| Cast asphalt + Insulation mat | Thickness 35-40mm |
| Overlay (hard concrete) | Unreinforced, thickness 0-25 mm. Probably executed for slope buildup. The overlay was delaminated and lacked adhesion to the structural concrete. |
| Structural concrete surface | Fine crack in the structural concrete, 0.1 mm. Delamination indication was directly adjacent to the crack. Delamination area approximately 0.1-0.2×0.95 m. |
| Concrete cover layer | 30 mm. measured with a cover meter |
| Other | Based on all window inspections, it is likely that localized corrosion exists on the reinforcement mesh beneath the crack area. Corrosion attacks in the window are probably not extensive as only a weak and localized delamination indication could be heard. |

The examinations of windows on the First floor reveal that the overlay intended for slope augmentation exhibits delimitation and deficient adhesion. Among the inspected windows, localized corrosion of reinforcement was detected in only one out of two instances. These areas are appraised as posing the greatest risk for reinforcement corrosion, particularly due to their low elevation coupled with high vehicular traffic. Preservation of the waterproofing layer over the floor slab is anticipated to curtail the extent of reinforcement corrosion conditions. This anticipation stems from the protective barrier against moisture ingress afforded to the upper surface, while the underside benefits from exposure to the controlled indoor environment.

### 3.1.2 Inspection on the Floor 2

As previously described, considering visual signs such as the extent of corrosion cracking, and concrete spalling, and also conducting the hammer test to diagnose delamination, two windows with dimensions of 1x1 m were opened on this floor, based on the visual condition for inspection. Window number one, as illustrated in Figure 3.6, was opened in the section where concrete spalling and surface cracks were present on the main beam and at the lower part.


**Figure 3.6:** Location of window F1 in the second floor from Afry reports.

Figures 3.7 depict the condition of rebars in the opened window.

**Figure 3.7:** Condition of the reinforcement in the Window F1 from Afry reports.

Information regarding the condition of concrete and rebars has been compiled in Table 3.5. As expected, given the width of existing cracks and the thickness of the concrete cover, the corrosion rate of rebars in this section is high.

**Table 3.5:** The measured parameters is related to window F1.

| Parameter | Measurement notes from examination of F1 |
|---|---|
| Overlay (hard concrete) | Thickness 12mm |
| Reinforcement $\phi 8, S100(upperlayer)$ | Corrosion level: 1 out of 9 bars rusted. 3 bars with severe reinforcement corrosion, locally 0 3 mm remaining. |
| Main reinforcement $\phi 16, S = 100$ | Corrosion level: 3 bars with remaining diameter of 14-15 mm. |
| Concrete Cover layer (including overlay) | Approximately 30-32 mm |
| Other | Cracking due to damage, approximately 0.1 mm. It is noteworthy that corrosion attacks on the reinforcement are worst adjacent to the cracks. |

Window F2 was positioned at a lower elevation next to a column and above a main beam. Its surface exhibited partial delamination, extending into an area that had previously undergone repairs, as illustrated in Figure 3.9


**Figure 3.8:** Location of window F2 from Afry reports.

Detailed findings from the measurements and examination conducted on F2 are outlined in Table 3.6

**Table 3.6:** The measured parameters with window F2.

| Parameter | Measurement notes from examination of F2 |
|---|---|
| Overlay (hard concrete) | Thickness 14mm |
| Reinforcement $\phi 8, S100(upperlayer)$ | Corrosion level: Several reinforcement bars with severe corrosion. At least 6 mm remaining diameter. |
| Main reinforcement $\phi 16, 1piese$ | Corrosion level: locally 12 mm remaining. |
| Concrete Cover layer (including overlay) | Approximately 30 mm |
| Other | Repair concrete did not fully encase the reinforcement (not underneath). |

The status of the bars can be observed in Figures 3.10 and 3.11.


**Figure 3.9:** Status of the bars in the window F2 from Afry reports.

**Figure 3.10:** Status of the bars in the window F2 from Afry reports.

The conducted window inspections confirm that the identified delamination areas and cracked surfaces at the top of the floor slabs are caused by reinforcement corrosion. Considering the nature of the corrosion attacks, it is highly likely that the damage is caused by chloride ingress. The inspection reveals severe corrosion attacks on the mesh reinforcement but also significant attacks on the main reinforcement. It cannot be ruled out that there are areas with even more severe corrosion attacks on the main reinforcement.

## 3.2 Case Study Two

The second case study focused on a six-story parking structure built in 2001. As a previous case study, in parking structures, chlorides can come into contact with concrete through de-icing salts brought in by vehicles during winter. The inspection revealed that chloride easily penetrated the concrete in areas with cracks, leading to reinforcement corrosion. The width of cracks decreased with increasing concrete depth, correlating with reduced chloride penetration. Chloride was identified to enter the parking structure through de-icing salts and might have been trapped during construction.

The report provided detailed information on chloride and its threshold limit. Crack widths were mostly over 1 millimeter, with the maximum width being 2.5 millimeters. The study explored the relationship between crack width and chloride permeability, indicating that wider cracks allowed more chloride penetration. Additionally, as the concrete depth increased, crack widths decreased, showing the influence of concrete cover thickness.

These findings underscore the importance of crack width and concrete depth in assessing chloride penetration and its impact on reinforcement corrosion. In this case, based on visual inspections and observation of some corrosion signs, sampling was conducted at various points on different floors to examine the depth of cracks and the chloride content present in concrete. The cracks are, in several instances, significant at the surface, exceeding 1 mm in width. The maximum crack width measured at core sample position 5:1 was 2.5 mm, as shown in Figure 3.11.


**Figure 3.11:** Crack width in different samples from Afry reports.

Collected data from core samples can be observed in Tables 3.7 and 3.8.

**Table 3.7:** Information related to different samples.

| Plan/numbering | Comment | Core length (mm) | Crack width on surface (mm) | Crack depth (mm) |
|---|---|---|---|---|
| 3:1 | Over crack | 75 | 0.3 | at 75 mm depth 0 mm, crack closes |
| 3:2 | Undamaged surface, high point | 75 | - | - |
| 3:3 | over crack | 50 | 0.2 | at 50 mm depth :crack width 0.1 mm |
| 5:1 | Over crack | 65 | 2.5 | core split,crack width not determinable at greater depth |
| 5:2 | Undamaged surface,high point.standing water nearby. | 65 | - | - |
| 6:1 | Undamaged surface,high point. | 65 | - | - |
| 6:2 | over crack,low point | 75 | 0.2 | at 55 mm depth 0 mm, crack closes |

**Table 3.8:** Chloride content through the depth of different samples.

| Label | Remarks | Chloride depth(mm) | Chloride of cement weight(%) | Cement content (%) |
|---|---|---|---|---|
| 3:1 | cracked | 10-20 | 0.51 | 18.2 |
| | | 40-50 | 0.36 | 18.6 |
| | | 60-70 | 0.38 | 22.4 |
| 3:2 | Uncracked | 10-20 | 0.39 | 22.7 |
| | | 40-50 | 0.03 | 16.0 |
| | | 60-70 | 0.02 | 19.0 |
| 3:3 | cracked | 10-20 | 0.54 | 21.9 |
| | | 40-50 | 0.42 | 18.1 |
| 5:1 | cracked | 10-20 | 0.59 | 27.0 |
| | | 40-50 | 0.36 | 17.1 |
| 5:2 | Uncracked | 10-20 | 0.91 | 26.4 |
| | | 40-50 | 0.40 | 24.8 |
| 6:1 | Uncracked | 10-20 | 0.19 | 26.4 |
| | | 40-50 | 0.08 | 25.2 |
| | | 60-70 | 0.04 | 23.4 |
| 6:2 | Cracked | 10-20 | 0.21 | 20.7 |
| | | 40-50 | 0.06 | 24.0 |
| | | 60-70 | 0.04 | 20.3 |

### 3.2.1 Summary

The presence of cracks in the floor slabs indicates durability issues, particularly due to the prospective risk of chloride-induced corrosion on the unbounded reinforcement. Examination of crack dimensions, both on the surface and through core sampling, indicates a reduction in crack width with increasing depth. While these cracks do not penetrate the entire thickness of the slab, they do extend to at least the unbounded reinforcement situated atop the floor slabs in certain instances. This condition facilitates the ingress of chloride-laden water into the reinforcement. Chloride testing confirms the infiltration of chloride into the floor slabs. Additionally, the analysis detailed in Table 3.8 reveals a decline in chloride levels with increasing depth, highlighting the effect of cover thickness. The impact of cracks and their width is also evident, as concrete with larger cracks exhibits higher chloride content compared to concrete with smaller cracks and uncracked sections. In areas without cracks, the chance of reinforcement corrosion is very low.

## 3.3 Case study 3

Case number three focused on studying a structure located near the sea in an outdoor environment, with part of it situated in the water, constructed for vehicular traffic. According to the common method in visual inspections, areas with damages such as cracks, and concrete spalling were initially examined, and in these points, the rebound hammer test was also conducted. Based on the initial inspections, in the area where the highest probability of corrosion existed, sampling was done for chloride surface area measurement, and additionally, a window was opened to further examine the condition of the rebars. In this examination, considering that corrosion materials may move due to dynamic loads and corrosion may not be evident at the site, an extra window was also opened near the intended location for further investigation.

### 3.3.1 Core Samples and Chloride Testing

The core samples were visually inspected after extraction. Based on the inspection, it was observed that the cracks in the harbor deck extended through the entire length of the core, reaching at least down to the reinforcement depth of 70 mm.

The measured cover thickness was around 70 mm for all windows. Chloride levels are generally low, ranging from 0.1% to 0.4% of the cement weight at the depth of the reinforcement, where the current risk of reinforcement corrosion is assessed as low to moderate. The testing indicates that chloride levels in cracks are generally higher than in uncracked concrete.

Figure 3.12 shows window F1 with results from chloride analyses for each core sample and depth. All chloride levels are low at the depth of reinforcement. Once again, the influence of concrete thickness is apparent here, as the chloride levels decrease with increased depth. Considering the chloride values on the surface of the rebars, the expectation of corrosion is significantly low.

| Window 1, Test 2, Uncracked | |
|---|---|
| Depth | Cl/cem-weight [%] |
| 10-25 | 0.3 |
| 25-50 | 0.1 |
| 50-60 | <0.1 |

| Window 1, Test 1, cracked | |
|---|---|
| Depth | Cl/cem-weight [%] |
| 10-25 | 0.4 |
| 25-50 | 0.3 |
| 50-60 | 0.1 |

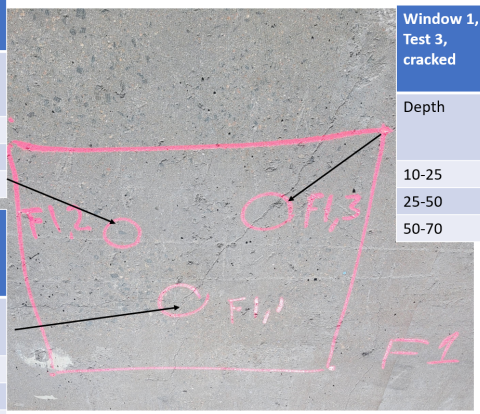


| Window 1, Test 3, cracked | |
|---|---|
| Depth | Cl/cem-weight [%] |
| 10-25 | 0.7 |
| 25-50 | 0.3 |
| 50-70 | 0.2 |

**Figure 3.12:** Chloride content through depth in window F1 from Afry reports.

The chloride content-to-cement ratio at the level of the rebar is of significant importance. According to the values presented in Figure 3.12, which are less than 0.4%, the probability of corrosion in the rebar is negligible. As shown in Figure 3.13 the reinforcement in window F1 was visibly unaffected, showing no signs of corrosion.

**Figure 3.13:** Reinforcement statement in window F1 from Afry reports.

Figure 3.14 shows window 2 with results from chloride analyses for each core sample and depth. For two positions, the ratio of chloride to cement at the rebar surfaces was 0.3-0.4%, which is assessed to pose a moderate risk of reinforcement corrosion. Additionally, the observed discoloration on the surface of the concrete, which may result from the reaction of corrosion products with water, further supports this probability.


**Figure 3.14:** Chloride content through depth in window F2 from Afry reports.

As expected, considering signs such as discoloration, the presence of cracks, and the measurement of the chloride-to-cement ratio, a reinforcing bar located at the level of a crack near sample F2.1 showed some pitting corrosion of a few millimeters, as shown in Figure 3.15 and Figure 3.16 Otherwise, the reinforcement was unaffected.


**Figure 3.15:** Bars status in window F2 from Afry reports.

**Figure 3.16:** Localised corrosion close to the cracks in window F2 from Afry reports.

A close-up of the crack extending below the level of the reinforcement is shown in Figure 3.17. The significance of the cracks is once again evident. A crack that has penetrated the depth of the concrete facilitates the access of harmful substances to the rebar, and corrosion has been observed at this location.

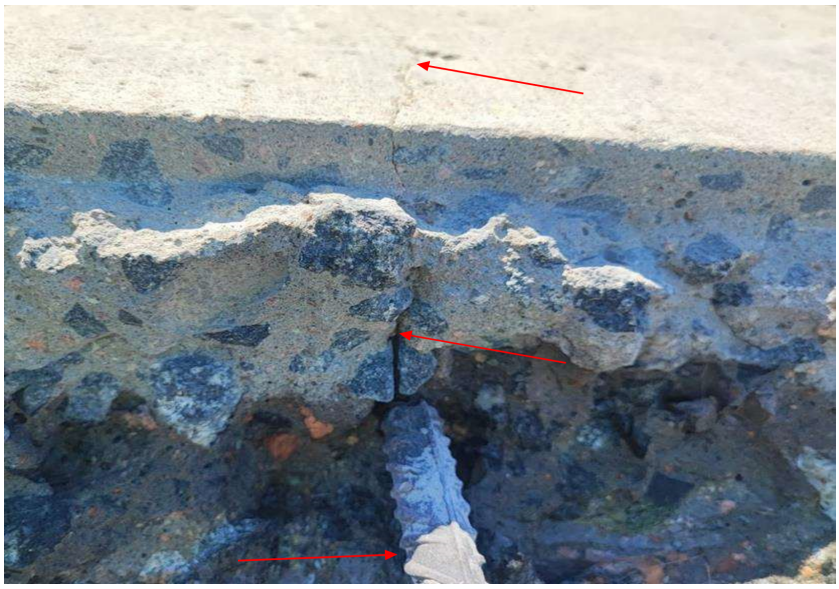

**Figure 3.17:** Close up of the crack extending to the bar surface from Afry reports.

Window 3 with results from chloride analyses for each core sample and depth is shown in Figure 3.18. All chloride levels are low at the depth of reinforcement therefore the probability of corrosion is negligible.

| Window 3, Test 1, cracked | |
|---|---|
| Depth | Cl/cem-weight [%] |
| 10-25 | 0.3 |
| 25-50 | 0.2 |
| 50-70 | 0.2 |

| Window 3, Test 2, cracked | |
|---|---|
| Depth | Cl/cem-weight [%] |
| 10-25 | 0.4 |
| 25-50 | 0.3 |
| 50-75 | 0.1 |

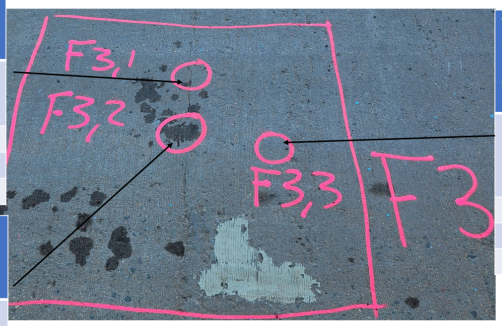


| Window 3, Test 3, uncracked | |
|---|---|
| Depth | Cl/cem-weight [%] |
| 10-30 | 0.4 |
| 30-60 | 0.1 |
| 60-87 | <0.1 |

**Figure 3.18:** Chloride content through depth in window F3 from Afry reports.

In window F3, the existence of cracks and their proximity to an area likely to experience corrosion warranted further investigation, prompting the opening of this section for closer inspection. Figure 3.19 included in the report shows no evidence of corrosion. This finding indicates that the cracks might have been caused by factors other than corrosion, as mentioned earlier.

**Figure 3.19:** The bars status in window F3 from Afry reports.

The results of the conducted chloride testing and crack width are presented in Tables 3.9 and 3.10. The results, as expected, show that chloride levels decrease as the depth within the concrete increases. This suggests that the thickness of the concrete cover plays a protective role in reducing chloride penetration. Additionally, there is a clear trend that larger cracks in the concrete are linked to higher chloride levels. This pattern supports the theory that the width of cracks and the thickness of the concrete cover affect how much chloride is found in concrete. The data collected from various samples confirm this relationship.

**Table 3.9:** Chloride content in samples in different depths.

| Sample | Test Depth (mm) | Estimated Chloride(%of cement weight) |
|---|---|---|
| F1 1:1 | 0-25 | 0.4 |
| F1 1:2 | 25-50 | 0.3 |
| F1 1:3 | 50-60 | 0.1 |
| F1 2:1 | 0-25 | 0.3 |
| F1 2:2 | 25-50 | 0.1 |
| F1 2:3 | 50-60 | <0.1 |
| F1 3:1 | 0-25 | 0.7 |
| F1 3:2 | 25-50 | 0.3 |
| F1 3:3 | 50-70 | 0.2 |
| F2 1:1 | 0-30 | 0.8 |
| F2 1:2 | 30-60 | 0.4 |
| F2 1:3 | 60-79 | 0.4 |
| F2 2:1 | 10-30 | 0.5 |
| F2 2:2 | 30-60 | 0.3 |
| F2 2:3 | 60-85 | 0.2 |
| F2 3:1 | 0-30 | 0.6 |
| F2 3:2 | 30-60 | 0.3 |
| F2 3:3 | 60-85 | 0.3 |
| F3 1:1 | 0-25 | 0.3 |
| F3 1:2 | 25-50 | 0.2 |
| F3 1:3 | 50-70 | 0.2 |
| F3 2:1 | 0-25 | 0.4 |
| F3 2:2 | 25-50 | 0.3 |
| F3 2:3 | 50-75 | 0.1 |
| F3 3:1 | 0-30 | 0.4 |
| F3 3:2 | 30-60 | 0.1 |
| F3 3:3 | 60-87 | <0.1 |

**Table 3.10:** Crack width in different samples.

| Sample | length (mm) | Diameter (mm) | Crack width (mm) |
|---|---|---|---|
| F1,1 | 60 | 45 | 0.2 |
| F1,2 | 60 | 45 | None |
| F1,3 | 70 | 45 | 0.2 |
| F2,1 | 79 | 45 | 0.3 |
| F2,2 | 85 | 45 | <0.1 |
| F2,3 | 85 | 45 | 0.2 |
| F3,1 | 70 | 45 | 0.3 |
| F3,2 | 75 | 45 | 0.2 |
| F3,3 | 87 | 45 | None |

## 3.4 iCAMM Method

Following a comprehensive site examination during visual inspections, areas exhibiting superficial damage, such as cracks and concrete spalling, are identified. To further assess the internal condition of structures, some non-destructive methods are employed in practical engineering. One of these methods is the Infrastructure Corrosion Assessment Magnetic Method (iCAMM), which is utilized to inspect the condition of rebars within concrete structures such as bridges and buildings. This method is predicated on the measurement of magnetic flux density, as expressed by the equation:

$$B = \frac{\Phi}{A} \tag{3.1}$$

Where:

- $B$ is the magnetic flux density,
- $\Phi$ is the magnetic flux, and
- $A$ is the area through which the flux is passing.

The iCAMM method comprises several critical steps to ensure a thorough assessment of ferromagnetic materials:

- **Magnetic Field Application:** The inspection begins with the application of a magnetic field to the ferromagnetic material, achieved using either permanent magnets or electromagnets. The specific nature and intensity of the magnetic field are tailored based on the characteristics of the structure under examination.
- **Detection of Magnetic Flux Leakage:** Fundamental to this method is the detection of magnetic flux leakage, a common indicator in magnetic testing methods. Corrosion or material loss disrupts the magnetic field, causing leakage detectable in areas of corrosion or pitting.
- **Data Analysis:** Data collected from detected magnetic flux leakages or other magnetic anomalies are rigorously analyzed to determine the corrosion's extent and location. This analysis typically involves advanced algorithms and software that generate visual maps highlighting affected areas.
- **Evaluation and Reporting:** The final phase involves evaluating the severity of detected corrosion and integrating these findings into a detailed report. This report informs maintenance strategies and potential further testing requirements.

The performance and accuracy of the iCAMM method were validated in an experimental study [26]. This study included a comparative analysis between iCAMM inspection results and laboratory 3D scanning of rebars. This comparison demonstrated the method's high precision in identifying areas with significant corrosion and cross-sectional loss.

In a separate study [25], they examined the condition of an existing bridge in one of the cities in Canada using this method. Visual inspections were conducted on this bridge in 2017, and areas prone to corrosion were identified based on observable changes such as discoloration, crack formation, and spalling. Furthermore, specific points were selected for sampling to measure the concrete quality, cover thickness, and determine its chloride content, as illustrated in Figures 3.20 and 3.21.

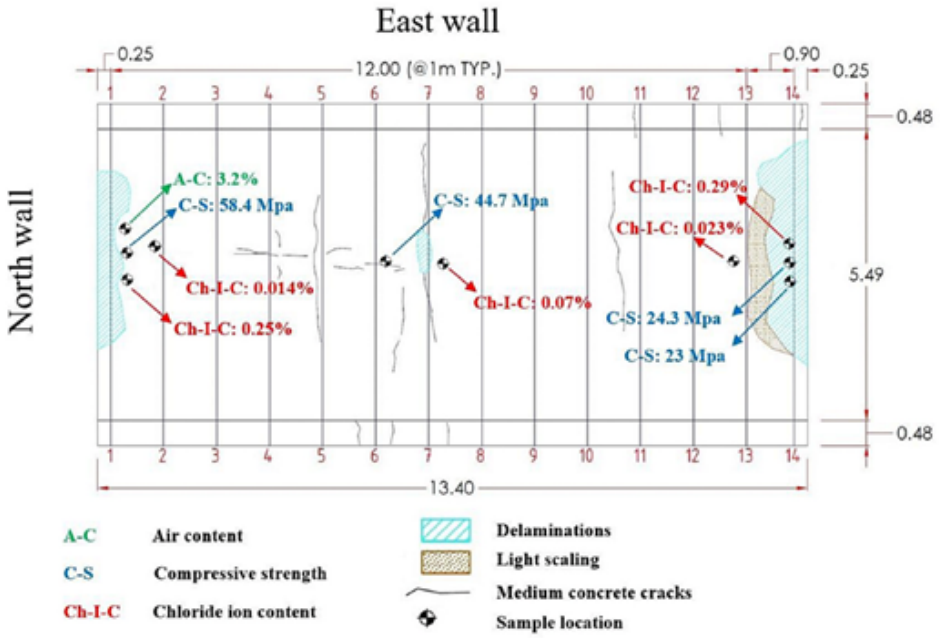


**Figure 3.20:** Surface deterioration on the top of slab from [25]

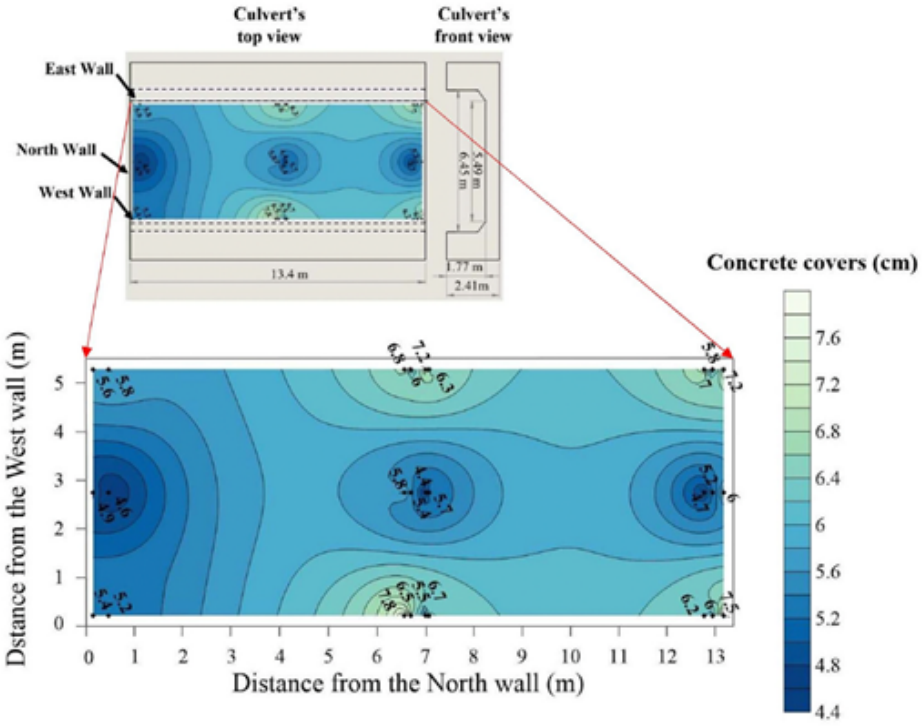


**Figure 3.21:** Measured concrete cover thickness in different places from [25]

As previously mentioned, several parameters influence the extent of corrosion, including concrete cover thickness, concrete quality, and rebar size [15]. Additionally, the presence of cracks and chloride levels also significantly affect corrosion rates [5]. The analysis of samples indicated that areas with thinner concrete covers, lower-quality concrete, and higher chloride content are more susceptible to corrosion. These observations are supported by results obtained from this method and are illustrated in Figure 3.22.

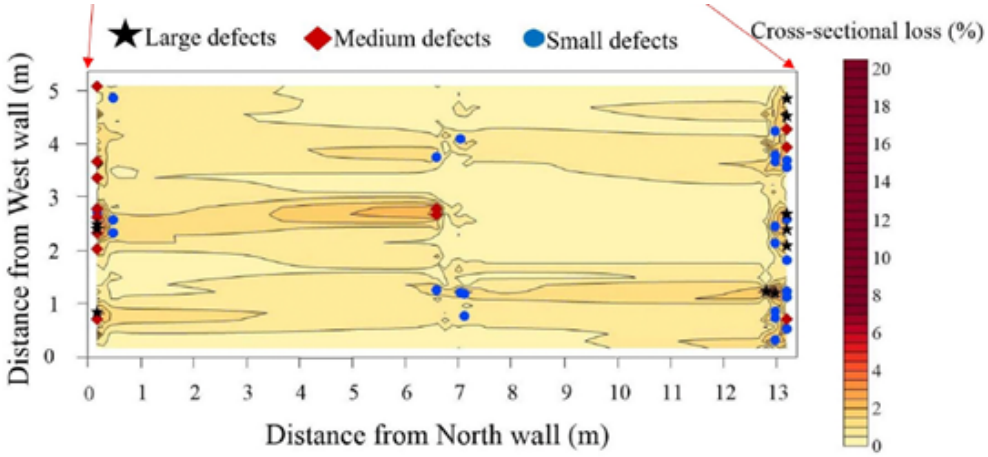


**Figure 3.22:** Different types of defects in the scanned area from [25]

As shown in Figure 3.22, Mosharafi et al.(2020) classified the damages into three categories based on the visual condition of the affected parts and the level of corro-

sion measured by the iCAMM method:

- Small defects, with the defects causing approximately a 4–7% loss in cross-sectional area.
- Medium defects, with the defects causing approximately a 7–10% loss in cross-sectional area.
- Large defects, with those defects causing greater than 10% loss in cross-sectional area.

As a result, considering the studies conducted on iCAMM method and the accuracy of its results, as well as the case study and sampling performed, the influence of parameters such as concrete quality, concrete cover thickness, and presence of cracks is once again clearly observable. In areas where these parameters indicated a high probability of corrosion, they were well correlated with the results obtained from iCAMM method.

## 3.5 Discussion

Based on the studies conducted in this section, it has been determined that most of these types of inspections are requested by the owner based on the structural conditions and the extent of the damages, except for bridges that fall under the responsibility of the Swedish Transport Administration and are required to be evaluated and inspected every six years according to their guidelines. There are no specific regulations mandating the inspection of structures at regular intervals. If periodic inspections were implemented as a guideline, it could aid in the prompt identification and rectification of damages, thereby extending the structure's service life.

One factor that accelerates the corrosion process and increases its extent is the environment in which the structure is located and the humidity level in that environment. This aspect is included in the Eurocode classification of exposure classes, suggesting that structures in more vulnerable environments should be inspected more frequently and at shorter intervals.

As expected, the type of loading also affects the rate of corrosion, with areas subjected to more dynamic loads exhibiting higher corrosion rates than other areas. This observation has also been noted in experimental studies, where one cause is the displacement of corrosion products and the reopening of cracks, exposing the rebar to harmful substances.

The thickness of the concrete cover and the surface coatings, such as asphalt or other materials, delay or sometimes prevent the penetration of harmful substances to the rebar surface, reducing the onset and extent of corrosion. However, increasing the concrete thickness can also have a counterproductive effect, leading to more transverse cracks and thereby increasing the pathways for harmful substances to reach the rebar.

In some structures, signs of corrosion have been repaired, and in such cases, tests like the hammer test are conducted, and sometimes windows are opened to ensure the condition of the rebar.

As mentioned, in some cases, multiple windows are opened close to each other to assess the condition of the rebar around the signs of corrosion, as sometimes corrosion occurs near the signs, but due to the movement of materials, the signs appear elsewhere.

The quality of the concrete is another factor that affects the rate of corrosion. As observed in experimental studies, higher-quality concrete has fewer pores, making it more difficult for corrosive substances to reach the rebar surface.

In practical engineering analysis, visual inspections play a crucial role in assessing the condition of concrete surfaces, focusing particularly on concrete discoloring, longitudinal cracks and their widths, concrete spalling, and delamination. These inspections critically evaluate the chloride content on the bar surface, which is directly correlated with the width of the cracks. Increased crack width typically leads to higher chloride levels, thus elevating the risk of rebar corrosion.

Accurately estimating the level of corrosion based solely on visual inspections is complex and requires consideration of various parameters such as concrete quality, rebar size, concrete cover thickness, loading type, environmental exposure, type of cement used, and even the age of the structure. Each of these factors significantly impacts the rate of corrosion.

Considering that factors such as water-to-cement ratio, exposure class, and loading type are consistent across the structures under study, the primary investigative focus is on the differences in concrete quality, concrete cover thickness, rebar size, and crack width. These elements are key in exploring the relationship between longitudinal crack width, concrete quality, concrete cover thickness, rebar size, and corrosion extent using available laboratory data.

# 4

# Relation between Corrosion-induced crack width and corrosion level

As mentioned before in visual inspections, the primary focus is on identifying changes in the physical characteristics of concrete, which leads to more detailed examinations of specific areas and assessments of the condition of the reinforcing bars. Given that such inspections lack precise tools for measuring certain parameters such as the chloride content of concrete without sampling, focus on parameters that are readily accessible and do not require precise instruments or laboratory samples. In this chapter previous studies are reviewed to find a relationship between the width of longitudinal cracks (as an indicator of rebar corrosion) and the level of corrosion. Furthermore, emphasis is placed on parameters like the thickness of the concrete cover, the diameter of the rebar, and the quality of the concrete.

## 4.1 Empirical relationships between Crack width and Corrosion level

Numerous studies have investigated the correlation between the width of longitudinal cracks and the extent of corrosion. In the following sections, several empirical relationships derived from these investigations are reviewed, and the data obtained from them. As previously mentioned, formulating a comprehensive relationship that accounts for all relevant parameters is challenging, and evaluating the impact of certain parameters in these studies is often not feasible, particularly given that many of them have been conducted using artificial methodologies. Additionally, considering the objective of this study, which is to estimate the corrosion level inside of the reinforced concrete based on surface changes.

In experimental studies conducted by Vidal et al (2007), two beams were exposed to chloride for 14 and 17 years. A chloride environment with wetting–drying cycles, generated using four sprayers located in the upper corner of a confined room. A linear expression between crack width and the corrosion level was defined according to Equation (4.1) characterized by R2 = 0.82 with experimental data.

$$W_c = K \cdot (\Delta A_s - \Delta A_{s0}) \tag{4.1}$$

where $K$ is constant equal to 0.0575 ;
$\Delta A_s$ Calculated based on equation (4.2);
$\Delta A_{s0}$ Calculated based on equation (4.3);

$$\Delta A_s = \frac{\pi}{4}(2\alpha x\phi_0 - \alpha^2 x^2) \tag{4.2}$$

where $\alpha$ is the pitting factor, this factor helps to describe how uneven or localized the corrosion is. A higher pitting factor indicates more localized corrosion, while a lower factor suggests a more uniform corrosion pattern. $\Delta As$ is the loss of the reinforcement cross-section $As$, and $\Delta As_0$ is the steel cross-section loss needed to generate concrete cover cracking, derived according to:

$$\Delta A_{s0} = A_s \left[1 - \left(1 - \frac{\alpha}{\phi_0}\left(7.53 + 9.32\frac{c}{\phi_0}\right) \times 10^{-3}\right)^2\right] \tag{4.3}$$

where $d$ is the bar diameter (mm);
$\alpha$ is the pit concentration factor, ( $\alpha = 2$, for homogeneous corrosion, $4 < \alpha < 8$, for localized corrosion);
$c$ is the cover concrete (mm);
$\Delta A_{s0}$ is the steel cross section loss ($mm^2$);
$As$ is the sound steel cross section ($mm^2$);

In the relationship obtained by Vidal et al.(2007), since both beams were made with the same concrete, the concrete characteristics were not considered. Zhang et al. (2010) studied a beam for a period of 23 years. The derived expression between the crack width $W_c$ (mm) and the average steel cross-section loss $\Delta A_{sm}$ ($mm^2$) as expressed in equation (4.4) is characterized by $R^2 = 0.85$:

$$W_c = 0.1916 \cdot \Delta A_{sm} + 0.164 \tag{4.4}$$

Khan et al.(2014) proposed a relationship based on one beam naturally corroded for 27 years. The beams were the same as Vidal et al. (2004) During the research, no links were found between the crack width induced by the longitudinal reinforcement corrosion and the one due to the stirrups' deterioration. Finally, Khan et al. (2014) revised the model proposed by Zhang et al. (2010) by means of the introduction of the diameter-to-cover ratio d/c. The proposed relationship in equation (4.5), characterized by R2 = 0.85, is:

$$Wc = 0.1916 \cdot \Delta A_{sm} \cdot \frac{d}{c} + 0.164 \tag{4.5}$$

where $d$ is the bar diameter (mm);
$c$ is the cover concrete (mm);
$\Delta Asm$ is the steel cross section loss ($mm^2$);

In the studies conducted by Andrade et al (2015), data related to experimental study with using an artificial method (impressed current) were collected. Andrade et al(2015), drawing from Torres' studies, proposed a relationship between the width of longitudinal cracks, and the ratio between average crack penetration and bar diameter, as shown in Equation (4.6), where the average crack penetration is derived according to Equation (4.7) by Torres et al.(2003)

$$W_{\max} = 15.863 \left( \frac{x_{\text{ave}} \cdot CT}{r_0} \right)^{0.928} \tag{4.6}$$

$$x_{\text{AVER}} = \frac{\Delta W \times 10^3}{\pi \phi L \rho_{\text{Fe}}} \tag{4.7}$$

Andrade et al (2015) calibrated this relationship by defining the new coefficient CT, which is shown in Equation (4.8). They focused on three parameters: the concrete cover thickness (mm), rebar size (mm), and concrete tensile strength (Mpa). Based on the experimental study, they defined alpha and beta constants as 0.63 and 1.41 MPa, respectively.

$$CT = \left( \alpha \cdot \frac{c}{\phi} \right)^{-\frac{\beta}{f_{ct}}} \tag{4.8}$$

By examining the previously presented relationships and conducting further studies, one can observe a form of evolution in these relationships that considers the impact of various parameters. In the initial relationships presented, the emphasis was primarily on the weight loss in rebar, which, given the measurement methods, has a high potential for error. This potential for error can affect the correlation of the relationships, which has not been considered in the provided relationships. In one of the latest equations presented by Andrade et al (2015), as shown in Equation 4.8, all measurable influencing parameters are considered. However, as mentioned in Chapter Two, other parameters such as loading and self-healing also play a role in the corrosion process. Due to their nature, these parameters require further studies to account for their long-term effects. Moreover, in the relationship presented by Andrade et al (2015), most samples were subjected to impressed current conditions, which accelerates the corrosion rate. Consequently, corrosion under these conditions is more pronounced than in natural settings. Therefore, the possibility of variations in the constant values of alpha and beta is quite high, necessitating more natural samples to obtain accurate values.

## 4.2 Data From previous studies

In this section, data from previous studies conducted using both natural and artificial methods are gathered for subsequent review and analysis. One of the studies in this area was conducted by Andrade et al(2015), who reviewed previous experimental works and proposed a relationship between crack width and corrosion level, as shown in Equation 4.6. The collected data by Andrade et al.(2015) is presented in Figure 4.1.

As observed, the data collected and calibrated by Andrade et al (2015) show significant variability. This variability can be attributed to several factors, as seen in Equation 4.7, where the crack width depends on the tensile strength of the concrete, rebar diameter, and cover thickness, all of which vary in the studies conducted. Another influential parameter is the impressed current, where higher currents increase the corrosion rate in the rebar, leading to increased internal pressure and consequently wider cracks [5]. According to various studies [4],[5],[6] on the effect of impressed current, lower currents are closer to natural corrosion conditions.

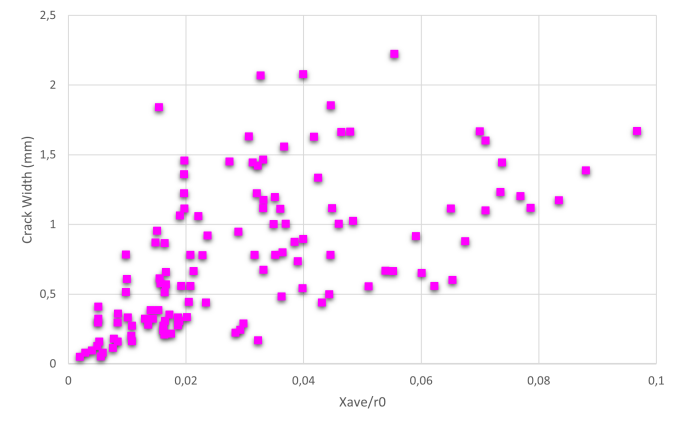


**Figure 4.1:** Crack width versus average corrosion penetration to initial bar diameter for artificial corrosion by Andrade et al [34]

Tahershamsi et al (2016) conducted another study on the relationship between crack width and rebar corrosion on existing samples from several beams taken from the Stallbacka bridge built in Sweden in 1979-81. In this study longitudinal cracks width were measured using a scaled electrometer with a 50x magnification microscope and the corrosion level of the extracted reinforcement bars was measured using the 3D scanning technique and Gravimetric measurements. The corrosion levels obtained from the gravimetric measurements ranged from 0.0 to 9.6 %, with standard deviations of ±0.51% for uncorroded bars with straight ribs and ±0.75% for those with skewed ribs. It was observed that the gravimetric weight loss method consistently yielded higher corrosion levels compared to the 3D scanning measurements for nearly all bars. This discrepancy can be attributed to the fact that small steel pieces detached from the original rebar during tensile testing, reducing the weight of the bars. This suggests the presence of horizontal or subsurface corrosion, which

cannot be measured or detected by 3D optical scanning. The result from this study is presented in Figure 4.2.

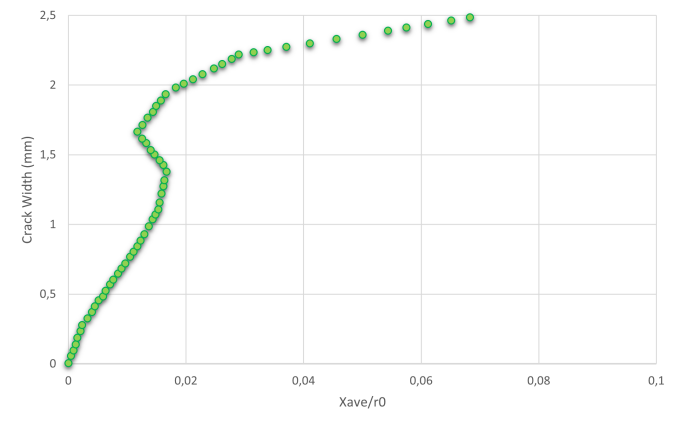


**Figure 4.2:** Crack width versus average corrosion penetration to initial bar diameter for natural corrosion 3D scanning [36]

Figure 4.3 present compiled data with artificial data by Tahershamsi et al (2016). The predicted corrosion from artificial method results exceeded that in natural conditions, which can be attributed to various factors such as impressed current rate, self-healing, freezing-thaw cycles, etc.

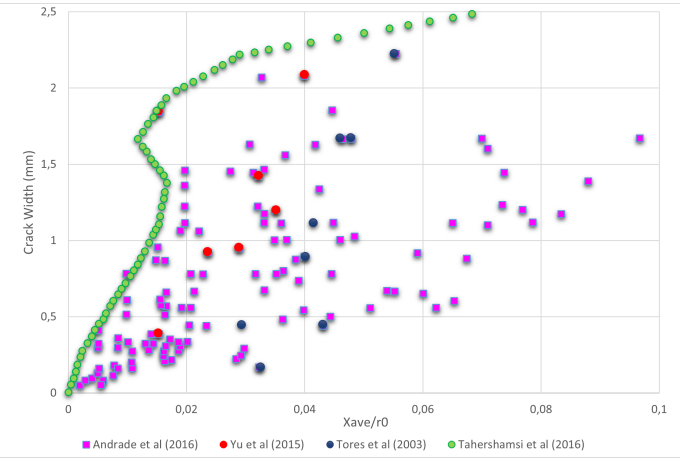


**Figure 4.3:** Crack width versus average corrosion penetration to initial bar diameter, compile of natural and artificial corrosion [36]

The data from experiments using artificial methods conducted by various studies have been collected in Figure 4.4. Due to differences in conditions and samples used, data scattering is observed, and it is not possible to extract a definite relationship from the data.

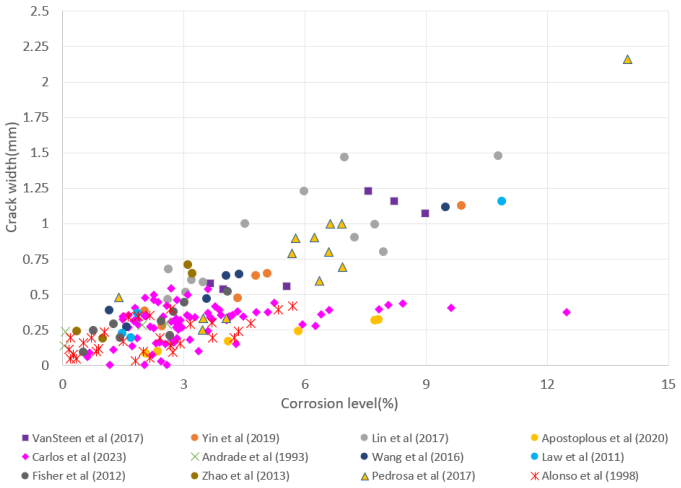


**Figure 4.4:** Crack width versus corrosion level for artificial corrosion

Also, the results obtained from the work carried out by Khan et al (2014), which studied samples exposed to chloride for 27 years under natural conditions, Yu et al (2015), and Torres et al (2003), were combined with the results from Tahershamsi et al (2016) as presented in Figure 4.5.

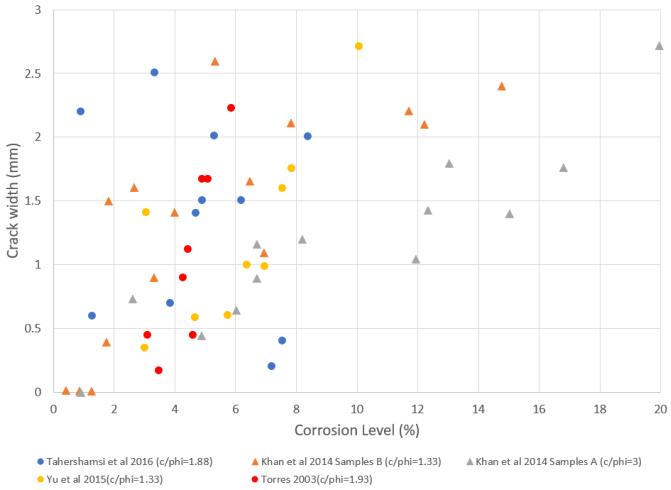


**Figure 4.5:** Crack width versus corrosion level for natural corrosion

In Figure 4.5, the level of corrosion increased with an increase in the ratio of cover thickness to bar diameter. This phenomenon could be attributed to the increased number of transverse cracks resulting from increased concrete thickness, thereby enhancing the pathways for corrosive substances to penetrate the reinforcement bars, ultimately leading to elevated corrosion levels.

Taking into account the results obtained by Tahershamsi et al (2016) all the collected data on crack width and corrosion level are shown in Figure 4.6.

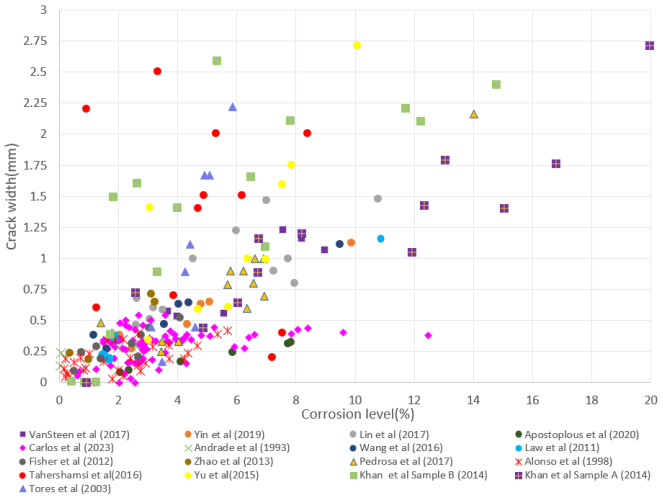


**Figure 4.6:** Crack width versus corrosion level, Compile of natural and artificial corrosion

As evidenced by the study results, due to the use of an impressed current, the corrosion level is overestimated in artificial conditions compared to natural conditions. Tahershamsi et al (2016) also noted this observation, suggesting it could depend on various parameters, such as self-healing and impressed current.

The experimental studies conducted have utilized different samples, each varying in parameters such as concrete quality, concrete cover thickness, rebar diameter, impressed current rate, and type of loading. These variations have each influenced the level of rebar corrosion to some extent. Given the focus of this study on estimating the level of rebar corrosion based on surface observations during visual inspections, the impact of parameters such as concrete cover thickness, concrete quality, and rebar diameter will be examined. Data from previous studies will be organized according to these parameters. To this end, hypotheses regarding how these parameters affect the level of corrosion are formulated.

Tahershamsi et al (2016) have studied natural samples and combined them with experimental studies, further data collection from both natural and artificial studies will continue in this study integrated with their data to increase the existing dataset and improve the statistical population. This approach aims to better examine the relationship between longitudinal crack width and the level of corrosion in rebar. The necessary information and data sources are listed in Table 4.1.

**Table 4.1:** Experimental (E) and Natural (N) specimens specifications

| Research | Concrete compression strength(Mpa) | Bar diameter (D)(mm) | Cover thick-ness(C) | C/D |
|---|---|---|---|---|
| Andrade et al. 1993 (E) | 35.5 | 16 | 20 | 1.25 |
| Rodriguez et al 1994 (E) | 40 | 16 | 24 | 1.5 |
| Alonso et al 1998 (E) | 22.9 | 16 | 62.4 | 3.9 |
| Torres et al 2003 (N) | 45 | 13 | 25 | 1.92 |
| El-Maadway et al 2005 (E) | 40.5 | 15 | 25 | 1.66 |
| Law et al 2011 (E) | 40 | 12 | 36 | 3 |
| Fisher et al 2012 (E) | 41 | 12,16 | 20 | 1.67,2.19 |
| Richard et al 2012 (E) | 44.7 | 20 | 25 | 1.25 |
| Zhao et al 2013 (E) | 41.9 | 18 | 66.6 | 3.7 |
| Khan et al 2014 sample B (N) | 45 | 12 | 16 | 1.33 |
| Khan et al 2014 sample A (N) | 45 | 16 | 48 | 3 |
| Yu et al 2015(N) | 45 | 12 | 16 | 1.33 |
| Wang et al 2016 (E) | 30 | 20 | 66 | 3.3 |
| Tahershamsi et al 2016 (N) | 45 | 16 | 30 | 1.88 |
| Pedrosa et al 2017 (E) | 37.5 | 16 | 40 | 2.5 |
| Lin et al 2017 (E) | 33 | 20 | 40 | 2 |
| Yin et al 2019 (E) | 44.9 | 14 | 40 | 2.85 |
| Apostopolous et al 2019 (E) | 30 | 16 | 25,40 | 1.6,2.5 |
| Van steen 2019 (E) | 44.9 | 12 | 69.6 | 5.8 |
| Berrocal et al 2022 (E) | 68.2 | 16 | 20 | 1.25 |

## 4.3 Proposed Hypothesis

In this section, hypotheses are proposed based on parameters accessible through visual inspections and the crack width. Given the significant data dispersion, the hypotheses will be examined across different crack width ranges. The maximum crack width is restricted to 3 mm, as exceeding this threshold can result in a transition of damage in the concrete from cracking to spalling or delamination. This approach involves categorizing the data by these parameters and identifying patterns within specific crack width intervals.

### 4.3.1 The First Hypothesis (Crack Width) :

Given the process of corrosion over time and the accumulation of corrosion products, it is expected that due to the accumulation of these materials and the increase in stress between the concrete and the reinforcement over time, the width of longitudinal cracks will increase. Therefore, Hypothesis one is defined based on this relationship, such that an increase in the level of corrosion leads to an increase in crack width, meaning that wider cracks indicate a higher level of corrosion.

### 4.3.2 The Second Hypothesis (Concrete quality) :

One of the pre-existing parameters is the quality of the concrete used in the structure. According to previous studies, as the quality of the concrete increases, the tensile strength of the concrete also increases. Consequently, a greater amount of corrosive materials is required to elevate the stress level on the concrete, leading to crack formation. Therefore, for cracks of equal width, it is expected that concrete with higher quality will exhibit more corrosion.

### 4.3.3 The Third Hypothesis (Cover thickness) :

Another influential and available parameter is the thickness of the concrete cover. The impact of concrete cover thickness can be observed in two distinct ways:

1. As the concrete cover thickness increases, the number of transverse cracks per unit length along the rebar due to bending increases, creating more pathways for corrosive materials to reach the rebar surface, thereby accelerating the corrosion process.
2. With an increase in concrete cover thickness, corrosive materials require more time to reach the concrete surface, thereby reducing the corrosion rate.

Given the points above, since the focus is on pitting corrosion, the area under investigation is limited, and the impact of the number of transverse crack repetitions is diminished. Therefore, item number two has been examined, and the hypothesis has been defined accordingly. For the same corrosion-induced crack width, a larger

cover thickness indicates a higher corrosion level.

### 4.3.4 The Forth Hypothesis (Bar diameter):

Another parameter affecting the corrosion level is the diameter of the rebar. According to previous studies, corrosion measured in percentage of cross-sectional area loss in rebar with a smaller diameter is greater due to its higher surface-to-volume ratio compared to rebar with a larger diameter. Therefore, it is expected that for the same corrosion-induced crack width, smaller bar diameters lead to higher corrosion levels.

### 4.3.5 The Fifth Hypothesis (Concrete cover to bar diameter ratio) :

Another parameter affecting the corrosion level is the ratio of concrete cover thickness to bar diameter. Increasing this ratio can occur due to an increase in the concrete cover thickness or a decrease in the rebar diameter, both of which are expected to result in increased corrosion level. Therefore, For the same corrosion-induced crack width, a higher ratio of the concrete cover to bar diameter indicates a higher corrosion level.

All hypotheses and the relevant parameters are detailed in Table 4.2. Subsequently, the obtained data and sample specifications will be presented in a three-dimensional format according to the defined hypotheses. The impact of each parameter concerning the hypotheses will then be analyzed to verify each of these hypotheses.

**Table 4.2:** Hypothesis

| Number | Name | Hypothesis | Parameters |
|---|---|---|---|
| 1 | Crack width | Higher corrosion-induced crack width, indicates higher corrosion level. | corrosion-induced crack width,corrosion level. |
| 2 | Concrete quality | For the same corrosion-induced crack width, a higher concrete quality indicates a higher corrosion level. | Concrete quality, corrosion-induced crack width,corrosion level. |
| 3 | Cover thickness | For the same corrosion-induced crack width, a larger cover thickness indicates a higher corrosion level. | Cover thickness, corrosion-induced crack width,corrosion level. |
| 4 | Bar diameter | For the same corrosion-induced crack width, a smaller bar diameter indicates a higher corrosion level. | Bar diameter, corrosion-induced crack width,corrosion level. |
| 5 | Concrete cover to bar diameter ratio | For the same corrosion-induced crack width, a higher ratio of the concrete cover to bar diameter indicates a higher corrosion level. | Concrete cover,bar diameter, corrosion-induced crack width,corrosion level. |

## 4.4 Testing of the hypotheses

In this section, the available data is analyzed to test the proposed hypotheses. For this purpose, three-dimensional and two-dimensional graphs are plotted based on each of the parameters influencing the hypotheses, and the resulting graphs are subsequently analyzed. For three-dimensional plotting, the Radial Basis Function (RBF) in Python was utilized. RBF interpolation is a method for fitting a smooth surface through scattered data points in multi-dimensional space. In the context of plotting, RBF interpolation takes a set of known data points (x, y, z), where x and y are coordinates and z is the value at those coordinates, and constructs a continuous surface that smoothly approximates the data. This interpolated surface can be plotted to visualize the spatial distribution and underlying trends of the data, providing a clearer and more comprehensive representation of the scattered data points.

### 4.4.1 Hypothesis 1:

The higher corrosion-induced crack width indicates a higher corrosion level.

Figure 4.7 presents the relationship between crack width and corrosion level, with a color gradient indicating varying levels of corrosion. When crack widths are small (below 0.5 mm), the corrosion levels are also low, typically under 5 percent. As crack widths increase, corrosion levels correspondingly rise, with widths between 0.5 mm and 1.5 mm associated with corrosion levels from approximately 5 to 15 percent. Further analysis reveals that as crack width exceeds 1.5 mm, there is a significant increase in corrosion levels, often above 15 percent. The most extreme data points, with crack widths approaching or exceeding 2.5 mm, correlate with the highest corrosion levels, above 25 percent.

Due to differences in parameters such as sample geometry and material properties, the distribution of data points indicates that the relationship between crack width and corrosion level is not strictly linear but shows a clear trend where larger crack widths generally correspond to higher corrosion levels. Upon detailed examination, the data supports the hypothesis that a higher corrosion-induced crack width correlates with a higher corrosion level.

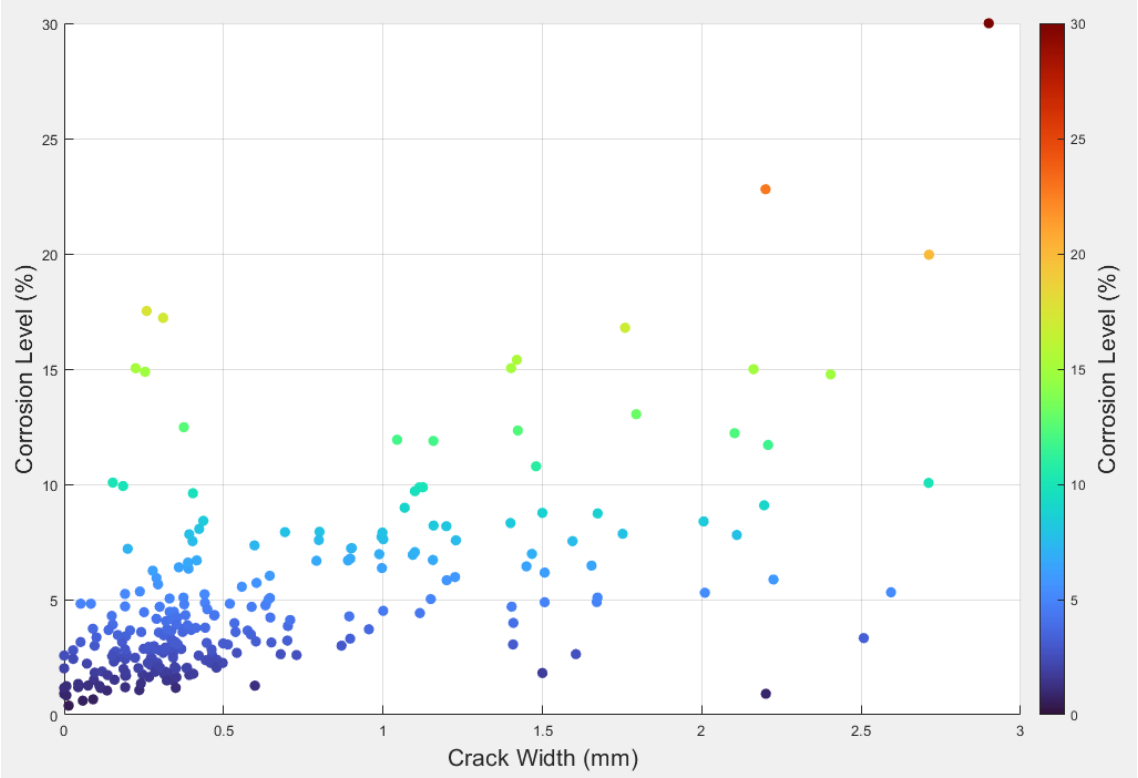


**Figure 4.7:** Crack width versus corrosion level

### 4.4.2 Hypothesis 2:

For the same corrosion-induced crack width, a higher concrete quality indicates a higher corrosion level.

The plots presented in Figure 4.8 display the relationship between concrete quality, crack width, and corrosion level. The hypothesis suggests a direct correlation between concrete quality and corrosion level for a given crack width. Upon detailed examination, it becomes evident that while there are regions in the graph where the corrosion level increases with higher concrete quality, this trend is not universally consistent across the entire dataset.

For crack widths between 0 to 0.5 mm, there is no clear pattern, with high corrosion levels seen in various concrete qualities. From 0.5 to 1.5 mm, a trend appears, higher concrete quality tends to have higher corrosion levels. For crack widths from 1.5 to 3 mm, The variation in concrete quality is too little to effectively test the hypothesis. In specific areas for crack widths between 0 to 0.5 mm, especially at lower concrete quality values, this correlation is less apparent. The corrosion level does not show a significant increase and sometimes remains constant or even decreases as concrete quality increases. One possible reason for this phenomenon could be related to the higher porosity in lower-quality concrete. This increased porosity allows the products of corrosion to initially fill these voids. Consequently, this delays the rise in stress within the concrete and the subsequent formation of cracks. Thus, despite a high level of corrosion, the width of the resulting cracks is less than anticipated.

Given the distribution of data points and the overall trend observed in the graph, it can be concluded that higher concrete quality doesn't correlate with higher corrosion levels for the same crack width. However, it should be noted that different parameters, such as sample geometry and material properties, may influence the results.

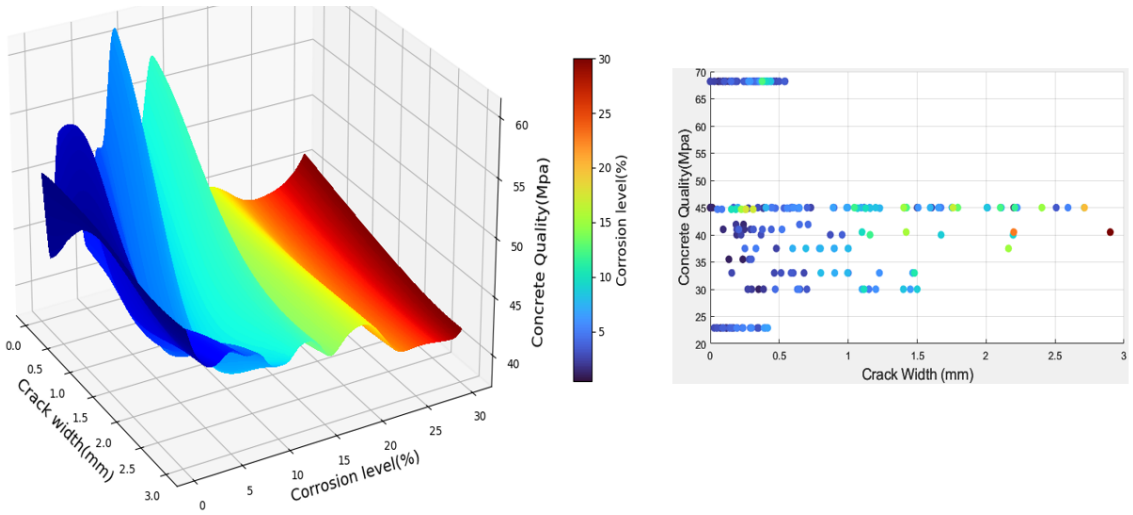


**Figure 4.8:** Crack width versus corrosion level versus Concrete Quality

### 4.4.3 Hypothesis 3:

For the same corrosion-induced crack width, a larger cover thickness indicates a higher corrosion level.

Figure 4.9 illustrates the interaction between cover thickness, crack width, and corrosion level. The hypothesis posits that for a given crack width, an increase in cover thickness should correspond to an increase in corrosion level. The visual representation in the graph provides substantial support for this hypothesis, particularly in the mid-range values of cover thickness (between 20 and 40). In these regions, the graph shows a clear trend where the corrosion level rises as the cover thickness increases, thereby supporting the hypothesis. However, at extreme values of cover thickness, the trend becomes less pronounced.

For 0 to 0.5 mm cracks, the data shows a mixed trend with no clear link between cover thickness and corrosion. In the 0.5 to 1.0 mm range, a trend starts to appear, where a thicker cover usually means more corrosion, but it is still somewhat scattered. For 1.0 to 2.0 mm cracks, the relationship is clearer and stronger, with a thicker cover consistently linked to higher corrosion. This trend is even more obvious in the 2.0 to 3.0 mm range, where thicker cover consistently shows more corrosion. Therefore, as cracks get bigger, the protective role of cover thickness decreases, leading to more corrosion, especially for larger cracks.

Overall, the graphs support the hypothesis, indicating that while larger cover thickness generally correlates with higher corrosion levels for the same crack width, there are limits to this trend.

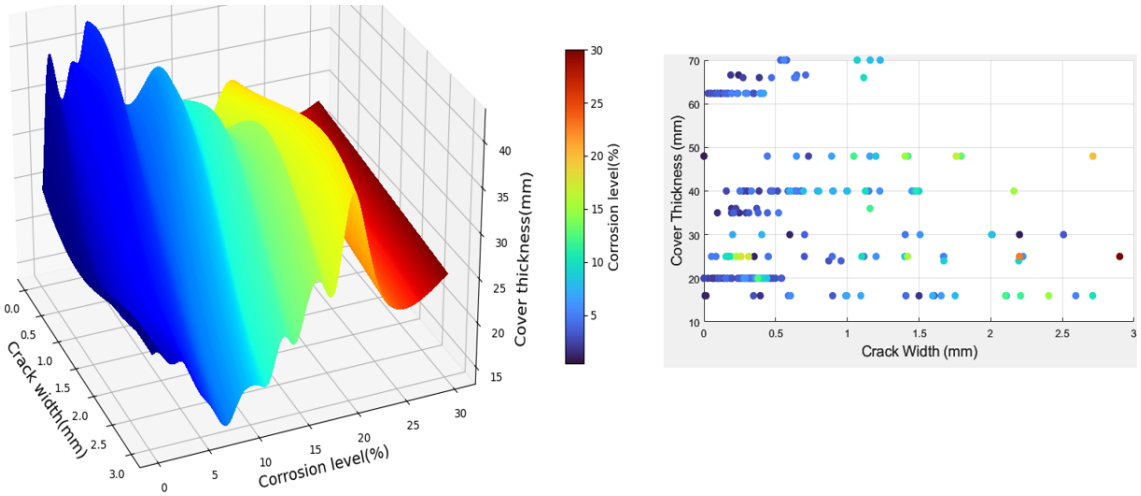


**Figure 4.9:** Crack width versus corrosion level versus Cover thickness

### 4.4.4 Hypothesis 4:

For the same corrosion-induced crack width, a smaller bar diameter indicates a higher corrosion level.

Figure 4.10 examines the relationship between bar diameter, crack width, and corrosion level. According to the hypothesis, smaller bar diameters should correspond to higher corrosion levels for a given crack width. The data shows a clear trend, as bar diameter increases, the corrosion level increases significantly, especially at mid to high crack widths.

Analyzing the graphs in more detail shows that for 0 to 0.5 mm crack width, the data shows that larger bar diameters often correspond to higher corrosion levels, which contradicts the initial hypothesis. In the 0.5 to 1.0 mm range, this trend continues, with larger bar diameters generally showing higher corrosion levels, further opposing the hypothesis. For 1.0 to 2.0 mm cracks, the relationship becomes even clearer, with higher corrosion levels consistently observed for larger bar diameters. This trend is most pronounced in the 2.0 to 3.0 mm range, where larger bar diameters are almost always associated with higher corrosion levels.

Overall, across all crack widths, the data indicates that larger bar diameters are linked to higher corrosion levels, clearly contradicting the hypothesis that larger diameters would mitigate corrosion. Since the observations consistently contradict the hypothesis, the hypothesis is proven false. Corrosion might not occur uniformly across the bar's surface. In larger bars, localized corrosion can lead to significant crack widths without drastically reducing the overall cross-sectional area, resulting in higher crack widths for lower relative corrosion levels compared to smaller bars.

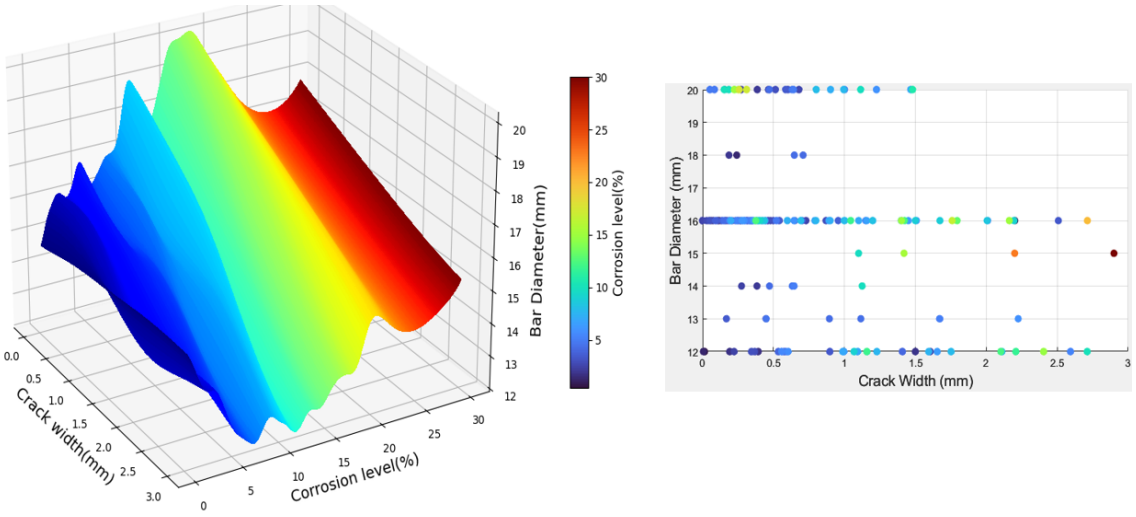


**Figure 4.10:** Crack width versus corrosion level versus Bar Diameter

### 4.4.5 Hypothesis 5:

For the same corrosion-induced crack width, a higher ratio of concrete cover to bar diameter indicates a higher corrosion level.

Figure 4.11 depicts the relationship between the concrete cover-to-bar diameter ratio, crack width, and corrosion level. The hypothesis asserts that an increased ratio should correspond to higher corrosion levels for a given crack width. The graph provides substantial evidence supporting this hypothesis, particularly in regions with higher ratios.

The data shows that as the ratio of concrete cover to bar diameter increases, the corrosion level also tends to increase, especially at mid-range crack widths.
While this trend holds true across most of the graph, there are some regions, particularly at very high ratios, where the increase in corrosion level is less pronounced.
The data shows that a higher ratio of concrete cover to bar diameter generally leads to higher corrosion levels across different crack widths.

For 0 to 0.5 mm cracks, the trend is scattered but suggests higher ratios mean more corrosion. In the 0.5 to 1 mm range, this trend becomes clearer, with higher ratios often linked to increased corrosion. For 1 to 2 mm cracks, the relationship is stronger and more consistent, showing higher ratios lead to more corrosion. This is most obvious in the 2 to 3 mm range, where higher ratios almost always mean higher corrosion.
Overall, the hypothesis is supported, higher ratios of concrete cover to bar diameter are linked to higher corrosion levels, especially as cracks get wider.

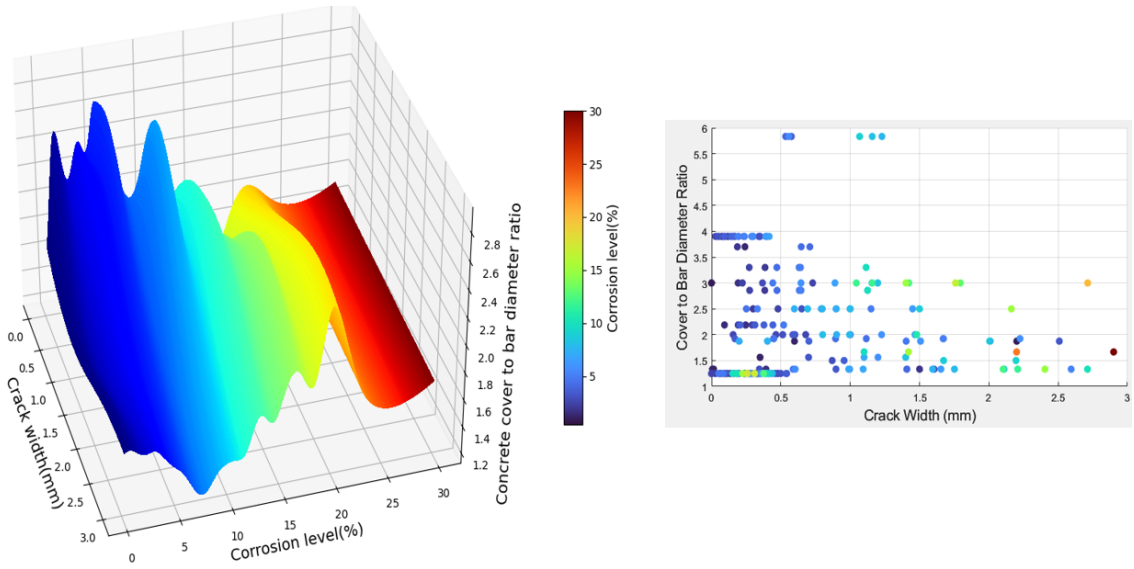


**Figure 4.11:** Crack width versus corrosion level versus Concrete cover to Bar Diameter ratio

## 4.5 Discussion

The analysis of the plots presented in Figures 4.7 to 4.11 provides valuable insights into the parameters influencing corrosion levels in reinforced concrete structures. The test of the hypotheses shows that corrosion behavior in reinforced concrete structures is complex. The analysis of the relationships between crack width, corrosion level, concrete quality, cover thickness, and bar diameter reveals complex interactions that challenge some initial hypotheses while supporting others. The results of the hypothesis testing are compiled in Table 4.3.

**Table 4.3:** Results of Testing Hypothesis

| Number | Name | Hypothesis | Testing Result |
|---|---|---|---|
| 1 | Crack width | Higher corrosion-induced crack width, indicates higher corrosion level. | Consistent |
| 2 | Concrete quality | For the same corrosion-induced crack width, a higher concrete quality indicates a higher corrosion level. | Contradicting |
| 3 | Cover thickness | For the same corrosion-induced crack width, a larger cover thickness indicates a higher corrosion level. | Consistent |
| 4 | Bar diameter | For the same corrosion-induced crack width, a smaller bar diameter indicates a higher corrosion level. | Contradicting |
| 5 | Concrete cover to bar diameter ratio | For the same corrosion-induced crack width, a higher ratio of the concrete cover to bar diameter indicates a higher corrosion level. | Consistent |

Higher crack widths consistently correlate with increased corrosion levels, confirming that wider cracks signify more severe corrosion. However, the hypothesis that for the same corrosion-induced crack width, a higher concrete quality indicates a higher corrosion level, was not supported, as increased porosity in lower-quality concrete may delay crack formation despite high corrosion.

In contrast, for the same corrosion-induced crack width thicker cover generally led to higher corrosion levels, suggesting that protective thicknesses may lose effectiveness as cracks widen. Larger bar diameters in the same corrosion-induced crack width were associated with higher corrosion levels, contrary to the expectation that smaller diameters would suffer more corrosion.

The ratio of concrete cover to bar diameter showed that for the same corrosion-induced crack width, higher ratios tended to increase corrosion levels. These findings highlight the complex nature of corrosion dynamics in reinforced concrete, underscoring the importance of considering multiple parameters in structural durability assessments.

# 5
# Conclusion

This study aimed to estimate the corrosion level of reinforced concrete bars through visual observations and surface changes in concrete during inspections. The initial phase examined the corrosion process and its influencing parameters, followed by an analysis of real cases to assess surface changes. The corrosion process is complex and depends on multiple parameters. Key parameters that are accessible during visual inspection include crack width, concrete quality, rebar diameter, concrete cover thickness, and the ratio of cover thickness to rebar diameter. These parameters are interconnected, and changes in one can affect the influence of others on the concrete.

Previous research indicated that longitudinal cracks on concrete surfaces are primarily due to rebar corrosion, with a correlation between crack width and rebar corrosion levels. Therefore, data from earlier studies on corrosion levels, longitudinal crack widths, and test sample characteristics (such as concrete quality, rebar diameter, concrete cover thickness, and the ratio of concrete cover thickness to rebar diameter) were collected.

Subsequently, hypotheses were developed based on the relationships between these parameters and the width of longitudinal cracks. The following conclusions were drawn based on the analysis of data according to the proposed hypotheses:

- Correlation Between Corrosion-induced Crack Width and Corrosion Level: Higher corrosion-induced crack widths generally correspond to higher corrosion levels, though the relationship is influenced by variations in sample geometry and material properties.

- Concrete Quality and Corrosion Level: For the same corrosion-induced crack width, higher concrete quality does not indicate higher corrosion levels, especially in lower-quality concrete where increased porosity delays crack formation.

- Cover Thickness and Corrosion Level: Larger cover thicknesses typically correlate with higher corrosion levels for the same corrosion-induce crack width at surface of concrete, supporting the hypothesis but with some limitations based on data variability.

- Bar Diameter and Corrosion Level: Smaller bar diameters do not correlate with higher corrosion levels; instead, larger bar diameters are linked to higher corrosion levels, contradicting the initial hypothesis.

• Concrete Cover-to-Bar Diameter Ratio: A higher ratio of concrete cover-to-bar diameter generally indicates higher corrosion levels, particularly as corrosion-induce crack widths increase.

One of the clear observations in the data analysis was the relationship between the width of longitudinal cracks and the extent of corrosion. However, finding a clear link between longitudinal crack width and corrosion levels is complicated and requires more studies that consider various parameters.

Most of the data came from experimental studies, previous research has shown, that experimental results often overestimate corrosion levels compared to natural conditions. To get more accurate results, it is necessary to study more natural samples. Human errors also play a big role in concrete performance and visual inspections. Mistakes during mixing, placing, and curing concrete can lead to variations in quality and cover thickness, affecting corrosion levels. Visual inspections are also sensetive to human error, possibly missing signs of corrosion or misjudging damage, leading to incorrect maintenance decisions.

The effects of the studied parameters on crack width and corrosion levels were well demonstrated in this project. These findings highlight the need for a broader approach to studying corrosion, considering more parameters and conditions.

For future research, the following suggestions are recommended:

• Parameter Study: Conduct a detailed analysis of parameters by modeling them with the finite element method, examining the impact of changing one parameter while keeping the others constant.
• Expand the Range of parameters: Examine more parameters like relative humidity, construction practices, and material properties to better understand corrosion in reinforced concrete.
• Field Studies: Conduct long-term field studies to compare experimental findings with natural conditions.
• Advanced Monitoring: Use advanced methods like non-destructive testing and predictive models to monitor corrosion in real time, aiding proactive maintenance.
• Improve Inspection Methods: Develop more reliable inspection methods using technology like drones or automated imaging systems to reduce human error and improve accuracy.
By addressing these areas, future studies can help create better strategies for corrosion in reinforced concrete structures, leading to safer and longer-lasting buildings and infrastructure.

# Bibliography

1. Al-Harthy, A. S.; Stewart, M. G.; Mullard, J. Concrete Cover Cracking Caused by Steel Reinforcement Corrosion. Mag. Concr. Res. 2011, 63 (9), 655–667. https://doi.org/10.1680/macr.2011.63.9.655.

2. Alonso, C.; Andrade, C.; Rodriguez, J.; Diez, J. M. Factors Controlling Cracking of Concrete Affected by Reinforcement Corrosion. Mater. Struct. 1998, 31 (7), 435–441. https://doi.org/10.1007/BF02480466.

3. Angst, U. Durable Concrete Structures: Cracks  Corrosion and Corrosion  Cracks. In Proceedings of the 10th International Conference on Fracture Mechanics of Concrete and Concrete Structures; IA-FraMCoS, 2019. https://doi.org/10.21012/FC10.233307.

4. Apostolopoulos, C. Alk.; Koulouris, K. F.; Apostolopoulos, A. Ch. Correlation of Surface Cracks of Concrete Due to Corrosion and Bond Strength (between Steel Bar and Concrete). Adv. Civ. Eng. 2019, 2019, 1–12. https://doi.org/10.1155/2019/3438743.

5. Axén, Å. Sprickor i anläggnings- konstruktioner av betong.

6. Benenato, A.; Ferracuti, B.; Imperatore, S.; Piero Lignola, G. Corrosion Level Estimation by Means of the Surface Crack Width. Constr. Build. Mater. 2022, 342, 128010. https://doi.org/10.1016/j.conbuildmat.2022.128010.

7. Berrocal, C. G.; Fernandez, I.; Rempling, R. The Interplay between Corrosion and Cracks in Reinforced Concrete Beams with Non-Uniform Reinforcement Corrosion. Mater. Struct. 2022, 55 (4), 120. https://doi.org/10.1617/s11527-022-01956-2.

8. Bossio, A.; Lignola, G. P.; Fabbrocino, F.; Monetta, T.; Prota, A.; Bellucci, F.; Manfredi, G. Nondestructive Assessment of Corrosion of Reinforcing Bars through Surface Concrete Cracks. Struct. Concr. 2017, 18 (1), 104–117. https://doi.org/10.1002/suco.201600034.

9. Cao, J.; Liu, L.; Zhao, S. Relationship between Corrosion of Reinforcement and Surface Cracking Width in Concrete. Adv. Civ. Eng. 2020, 2020, 1–14. https://doi.org/10.1155/2020/7936861.

10. Chang, L.-Z.; Thorsson, J.; Lundgren, K. 3D Modelling of the Interaction be-

tween Bending and Corrosion-Induced Cracks in Reinforced Concrete Beams. Constr. Build. Mater. 2024, 411, 134272.
https://doi.org/10.1016/j.conbuildmat.2023.134272.

11. Chen, E.; Berrocal, C. G.; Löfgren, I.; Lundgren, K. Correlation between Concrete Cracks and Corrosion Characteristics of Steel Reinforcement in Pre-Cracked Plain and Fibre-Reinforced Concrete Beams. Mater. Struct. 2020, 53 (2), 33.
https://doi.org/10.1617/s11527-020-01466-z.

12. Coccia, S.; Imperatore, S.; Rinaldi, Z. Influence of Corrosion on the Bond Strength of Steel Rebars in Concrete. Mater. Struct. 2016, 49 (1–2), 537–551.
https://doi.org/10.1617/s11527-014-0518-x.

13. El Maaddawy, T. A.; Soudki, K. A. Effectiveness of Impressed Current Technique to Simulate Corrosion of Steel Reinforcement in Concrete. J. Mater. Civ. Eng. 2003, 15 (1), 41–47. https://doi.org/10.1061/(ASCE)0899-1561(2003)15:1(41).

14. Fernandez, I.; Herrador, M. F.; Marí, A. R.; Bairán, J. M. Ultimate Capacity of Corroded Statically Indeterminate Reinforced Concrete Members. Int. J. Concr. Struct. Mater. 2018, 12 (1), 1-14. https://doi.org/10.1186/s40069-018-0229-y.

15. Hernández, Y.; de Rincón, O.; Torres, A.; Delgado, S.; Rodríguez, J.; Morón, O. Reinforcement Corrosion Rate and Crack Width Relationship in Concrete Beams Exposed to Simulated Marine Environment. 2016, 6 (3).
https://doi.org/10.21041/ra.v6i3.152.

16. Hong, S.; Zheng, F.; Shi, G.; Li, J.; Luo, X.; Xing, F.; Tang, L.; Dong, B. Determination of Impressed Current Efficiency during Accelerated Corrosion of Reinforcement. Cem. Concr. Compos. 2020, 108, 103536.
https://doi.org/10.1016/j.cemconcomp.2020.103536.

17. Imperatore, S.; Rinaldi, Z. Cracking in Reinforced Concrete Structures Damaged by Artificial Corrosion: An Overview. Open Constr. Build. Technol. J. 2019, 13 (1), 199–213.https://doi.org/10.2174/1874836801913010199.

18. Jamali, A.; Angst, U.; Adey, B.; Elsener, B. Modeling of Corrosion-Induced Concrete Cover Cracking: A Critical Analysis. Constr. Build. Mater. 2013, 42, 225–237.
https://doi.org/10.1016/j.conbuildmat.2013.01.019.

19. Khan, I.; François, R.; Castel, A. Prediction of Reinforcement Corrosion Using Corrosion Induced Cracks Width in Corroded Reinforced Concrete Beams. Cem. Concr. Res. 2014, 56, 84–96. https://doi.org/10.1016/j.cemconres.2013.11.006.

20. Korec, E.; Jirásek, M.; Wong, H. S.; Martínez-Pañeda, E. A Phase-Field Chemo-Mechanical Model for Corrosion-Induced Cracking in Reinforced Concrete. Constr. Build. Mater. 2023, 393, 131964. https://doi.org/10.1016/j.conbuildmat.2023.131964.

21. Lin, H.; Zhao, Y.; Ožbolt, J.; Reinhardt, H.-W. Bond Strength Evaluation of Corroded Steel Bars via the Surface Crack Width Induced by Reinforcement Corrosion. Eng. Struct. 2017, 152, 506–522. https://doi.org/10.1016/j.engstruct.2017.08.051

22. Li W, Liu W, Wang S (2017) The effect of crack width on chloride-induced corrosion of steel in concrete. Adv Mater Sci Eng. https://doi.org/10.1155/2017/3968578.

23. Mak, M. W. T.; Desnerck, P.; Lees, J. M. Correlation between Surface Crack Width and Steel Corrosion in Reinforced Concrete. MATEC Web Conf. 2018, 199, 04009. https://doi.org/10.1051/matecconf/201819904009.

24. Mohammed, T. U.; Otsuki, N.; Hisada, M.; Shibata, T. Effect of Crack Width and Bar Types on Corrosion of Steel in Concrete. J. Mater. Civ. Eng. 2001, 13 (3), 194–201. https://doi.org/10.1061/(ASCE)0899-1561(2001)13:3(194).

25. Mosharafi, M.; Mahbaz, S. B.; Dusseault, M. B. Bridge Deck Assessment Using Infrastructure Corrosion Assessment Magnetic Method (iCAMMTM) Technology, a Case Study of a Culvert in Markham City, Ontario, Canada. NDT E Int. 2020, 116, 102356. https://doi.org/10.1016/j.ndteint.2020.102356.

26. Mosharafi, M.; Mahbaz, S. B.; Dusseault, M. B.; Vanheeghe, P. Magnetic Detection of Corroded Steel Rebar: Reality and Simulations. NDT E Int. 2020, 110, 102225. https://doi.org/10.1016/j.ndteint.2020.102225.

27. Nasser, H.; Van Steen, C.; Vandewalle, L.; Verstrynge, E. An Experimental Assessment of Corrosion Damage and Bending Capacity Reduction of Singly Reinforced Concrete Beams Subjected to Accelerated Corrosion. Constr. Build. Mater. 2021, 286, 122773. https://doi.org/10.1016/j.conbuildmat.2021.122773.

28. Otieno, M. B.; Alexander, M. G.; Beushausen, H.-D. Corrosion in Cracked and Uncracked Concrete – Influence of Crack Width, Concrete Quality and Crack Reopening. Mag. Concr. Res. 2010, 62 (6), 393–404. https://doi.org/10.1680/macr.2010.62.6.393.

29. Poursaee, A.; Hansson, C. M. The Influence of Longitudinal Cracks on the Corrosion Protection Afforded Reinforcing Steel in High Performance Concrete. Cem. Concr. Res. 2008, 38 (8–9), 1098–1105. https://doi.org/10.1016/j.cemconres.2008.03.018.

30. Poursaee, A.; Ross, B. The Role of Cracks in Chloride-Induced Corrosion of Carbon Steel in Concrete—Review. Corros. Mater. Degrad. 2022, 3 (2), 258–269. https://doi.org/10.3390/cmd3020015.

31. Robuschi, S. Natural Corrosion in Reinforced Concrete Structures. https://research.chalmers.se/en/publication/526958.

32. Robuschi, S . Oskar Larsson Ivanov . Mette Geiker . Ignasi Fernandez .Karin

Lundgren(2022) Impact of cracks on distribution of chloride-induced reinforcement corrosion. https://link.springer.com/article/10.1617/s11527-022-02085-6

33. Robuschi, S.; Ivanov, O. L.; Geiker, M.; Fernandez, I.; Lundgren, K. Impact of Cracks on Distribution of Chloride-Induced Reinforcement Corrosion. Mater. Struct. 2023, 56 (1), 7. https://doi.org/10.1617/s11527-022-02085-6.

34. Świt, G.; Krampikowska, A.; Tworzewski, P. Non-Destructive Testing Methods for In Situ Crack Measurements and Morphology Analysis with a Focus on a Novel Approach to the Use of the Acoustic Emission Method. Materials 2023, 16 (23), 7440. https://doi.org/10.3390/ma16237440.

35. Tahershamsi, M. Structural Effects of Reinforcement Corrosion in Concrete Structures. https://research.chalmers.se/en/publication/239743.

36. Tahershamsi, M.; Fernandez, I.; Lundgren, K.; Zandi, K. Investigating Correlations between Crack Width, Corrosion Level and Anchorage Capacity. Struct. Infrastruct. Eng. 2017, 13 (10), 1294–1307. https://doi.org/10.1080/15732479.2016.1263673.

37. Van Steen, C.; Verstrynge, E.; Wevers, M.; Vandewalle, L. Assessing the Bond Behaviour of Corroded Smooth and Ribbed Rebars with Acoustic Emission Monitoring. Cem. Concr. Res. 2019, 120, 176–186. https://doi.org/10.1016/j.cemconres.2019.03.023.

38. Vidal, T.; Castel, A.; François, R. Analyzing Crack Width to Predict Corrosion in Reinforced Concrete. Cem. Concr. Res. 2004, 34 (1), 165–174. https://doi.org/10.1016/S0008-8846(03)00246-1.

39. Vidal, T.; Castel, A.; François, R. Corrosion Process and Structural Performance of a 17 Year Old Reinforced Concrete Beam Stored in Chloride Environment. Cem. Concr. Res. 2007, 37 (11), 1551–1561. https://doi.org/10.1016/j.cemconres.2007.08.004.

40. Wang, L.; Yi, J.; Xia, H.; Fan, L. Experimental Study of a Pull-out Test of Corroded Steel and Concrete Using the Acoustic Emission Monitoring Method. Constr. Build. Mater. 2016, 122, 163–170. https://doi.org/10.1016/j.conbuildmat.2016.06.046.

41. Yu, L.; François, R.; Dang, V. H.; L'Hostis, V.; Gagné, R. Distribution of Corrosion and Pitting Factor of Steel in Corroded RC Beams. Constr. Build. Mater. 2015, 95, 384–392. https://doi.org/10.1016/j.conbuildmat.2015.07.119.

42. Pettersson, K. (n.d.). Chloride threshold values in reinforced concrete. Cement och Betong Institutet, 100 44 Stockholm, Sweden.https://portal.research.lu.se/files/5608656/4146340.pdf.

43. Bridge and Tunnel Management Manuals (BaT-Man) from Sweden Trafikverket agency. https://batman.trafikverket.se.